AWARD NUMBER: W81XWH-17-2-0009

TITLE: Novel Anti-Fibrotic Strategies In The Targeted Treatment And Prevention Of Post-Traumatic Ho And Enhancement Of Post-Traumatic Tissue Regeneration

PRINCIPAL INVESTIGATOR: Leon Nesti, MD, PhD, COL, MC USA

RECIPIENT: Henry M. Jackson Foundation
6720A Rockledge Drive Suite 100
Bethesda, MD 20817-1891

REPORT DATE: September 2021

TYPE OF REPORT: Final

PREPARED FOR: U.S. Army Medical Research and Materiel Command
Fort Detrick, Maryland 21702-5012

REPORT DOCUMENTATION PAGE

Form Approved
OMB No. 0704-0188

1. REPORT DATE:	**2. REPORT TYPE**	**3. DATES COVERED**
SEPTEMBER 2021	Final	15MAY2017 - 14MAY2021

4. TITLE AND SUBTITLE:
:

Novel Anti-Fibrotic Strategies In The Targeted Treatment And Prevention Of Post-Traumatic Ho And Enhancement Of Post-Traumatic Tissue Regeneration

5a. CONTRACT NUMBER
W81XWH-17-2-0009

5b. GRANT NUMBER
Log # BA 150280

5c. PROGRAM ELEMENT NUMBER

6. AUTHOR(S)
Leon Nesti, MD, PhD; e-mail: leon.nesti@usuhs.edu
Jaira Ferreira de Vasconcellos, PhD; e-mail: vasconjf@jmu.edu

5d. PROJECT NUMBER

5e. TASK NUMBER

5f. WORK UNIT NUMBER

7. PERFORMING ORGANIZATION NAME(S) AND ADDRESS(ES)

Henry M. Jackson Foundation
6720A Rockledge Drive Suite 100
Bethesda, MD 20817-1891

8. PERFORMING ORGANIZATION REPORT NUMBER

9. SPONSORING / MONITORING AGENCY NAME(S) AND ADDRESS(ES)

U.S. Army Medical Research and Development Command
Fort Detrick, Maryland 21702-5012

10. SPONSOR/MONITOR'S ACRONYM(S)

11. SPONSOR/MONITOR'S REPORT NUMBER(S)

12. DISTRIBUTION / AVAILABILITY STATEMENT

Approved for Public Release; Distribution Unlimited

13. SUPPLEMENTARY NOTES

14. ABSTRACT

Neuromusculoskeletal injuries sustained in recent military conflicts have been notable for their number and complexity. Post-traumatic heterotopic ossification (HO) is the development of bone in the soft tissues and it is a significant sequela of these traumatic wounds occurring in approximately 60-70% of the war wounded. HO is the end product of a deranged fibroproliferative healing response and can render the extremity disfigured, painful and nonfunctional. Our group has studied this condition in combat related injuries at the cell and molecular level for the greater part of the last decade. In addition to identifying a progenitor cell population involved in this healing response, we have also identified TGF-beta mediated tissue fibrosis to be one of the key initial steps in the pathogenesis of HO and that dysregulation of the SMAD3 intracellular signaling protein in conjunction with a fibrotic microenvironment to be a central feature of the bone forming process.

15. SUBJECT TERMS

NONE LISTED

16. SECURITY CLASSIFICATION OF:			**17. LIMITATION OF ABSTRACT**	**18. NUMBER OF PAGES**	**19a. NAME OF RESPONSIBLE PERSON** USAMRMC
a. REPORT	**b. ABSTRACT**	**c. THIS PAGE**	Unclassified	46	**19b. TELEPHONE NUMBER** *(include area code)*
Unclassified	Unclassified	Unclassified			

Standard Form 298 (Rev. 8-98)
Prescribed by ANSI Std. Z39.18

TABLE OF CONTENTS

1. INTRODUCTION:

Current combat operations yield large numbers of traumatic neuromuscular injuries. As a consequence of these battlefield injuries traumatized muscle is intimately associated with the development of post-traumatic heterotopic ossification (HO). To identify a treatment strategy for HO it is necessary to understand the details of the process by which bone forms in muscle tissue. Despite extensive study, much of the cellular and molecular mechanisms underlying HO are still unknown.

What is known is that following combat trauma, wound closure is often delayed, leading to sub-optimal healing. While modulation of the local inflammatory response following injury is essential for wound healing and repair, severe traumatic injuries appear to initiate an over-exuberant response, thus compromising efficient wound healing & tissue regeneration. As a result of the chronic inflammation in the wound, endogenous tissue regeneration mechanisms are overshadowed by a generalized healing response that leads to formation of scar tissue. Fibrosis therefore limits the functional regeneration of the musculoskeletal tissues. Further, tissue fibrosis appears to be a salient feature in the HO lesion. Repeated anecdotal surgical observations have linked areas of abundant fibrotic scarring within the wound to an increased chance of HO formation. Fibrosis therefore appears to be an intermediate step in the onset of HO in a way that is not understood. It is possible that regions of fibrosis convert directly to bone. Additionally, it is possible that regions of fibrosis contribute osteogenic signals that drive neighboring cells to proceed down a bone-forming pathway. It can be predicted that any reduction in fibrosis should lead to a reduction in HO severity. Therefore, an appropriate treatment strategy for HO would therefore be to suppress fibrosis and promote the endogenous mechanisms of tissue repair. Ultimately, a timely administration of an effective HO prophylaxis to wounded soldiers in theater or soon thereafter could eliminate ectopic bone-related complications in blast amputation stumps and expedite rehabilitation, prosthetic limb use, and a return to productive life. Depending upon the efficacy-safety balance of the specific HO prophylaxis, it may be administered to all injured soldiers or only those at high risk for HO.

Over the past several years our lab has examined the cells, the molecular signals and the cellular scaffolds that are present in the wound-healing environment. We have identified a population of primary mesenchymal progenitor cells (MPCs) harvested from debrided human muscle tissue. These cells which are capable of differentiating down multiple pathways including bone and cartilage. MPCs have the potential to modulate differentiation due to their expression of multiple cytokines and growth factors. For example, they express TGFβ1, TGF 3, IL-10, GDF10 and BDNF at elevated levels compared to mesenchymal stem cells derived from human bone marrow. Consistent with this data, tissue samples from traumatized muscle also display elevated TGFβ1, TGF 3, IL-10, and BDNF, compared to normal muscle. Given the capacity of MPCs to undergo osteogenesis and to express cytokines and growth factors, it is likely that these MPCs play a critical role in both fibrosis and HO formation. We have therefore used these MPCs as a platform onto which we hope to rationally generate a treatment strategy for HO. In addition, we have made use of a recently generated rat model for post-traumatic HO, which very closely mimics that seen in wounded veterans. We have combined these in vitro and in vivo approaches

to identify a potential novel target for trauma-mediated muscle fibrosis that could block the formation of HO and potentially aid in muscle regeneration.

2. KEYWORDS:

Heterotopic ossification (HO), mesenchymal progenitor cells (MPCs), fibrosis, trauma

3. ACCOMPLISHMENTS:

Current combat operations yield large numbers of traumatic neuromuscular injuries. As a consequence of these battlefield injuries traumatized muscle is intimately associated with the development of post-traumatic heterotopic ossification (HO). To identify a treatment strategy for HO it is necessary to understand the details of the process by which bone forms in muscle tissue. Despite extensive study, much of the cellular and molecular mechanisms underlying HO are still unknown.

What is known is that following combat trauma, wound closure is often delayed, leading to sub-optimal healing. While modulation of the local inflammatory response following injury is essential for wound healing and repair, severe traumatic injuries appear to initiate an over-exuberant response, thus compromising efficient wound healing & tissue regeneration. As a result of the chronic inflammation in the wound, endogenous tissue regeneration mechanisms are overshadowed by a generalized healing response that leads to formation of scar tissue. Fibrosis therefore limits the functional regeneration of the musculoskeletal tissues. Further, tissue fibrosis appears to be a salient feature in the HO lesion. Repeated anecdotal surgical observations have linked areas of abundant fibrotic scarring within the wound to an increased chance of HO formation. Fibrosis therefore appears to be an intermediate step in the onset of HO in a way that is not understood. It is possible that regions of fibrosis convert directly to bone. Additionally, it is possible that regions of fibrosis contribute osteogenic signals that drive neighboring cells to proceed down a bone-forming pathway. It can be predicted that any reduction in fibrosis should lead to a reduction in HO severity. Therefore, an appropriate treatment strategy for HO would therefore be to suppress fibrosis and promote the endogenous mechanisms of tissue repair. Ultimately, a timely administration of an effective HO prophylaxis to wounded soldiers in theater or soon thereafter could eliminate ectopic bone-related complications in blast amputation stumps and expedite rehabilitation, prosthetic limb use, and a return to productive life. Depending upon the efficacy-safety balance of the specific HO prophylaxis, it may be administered to all injured soldiers or only those at high risk for HO.

Over the past several years our lab has examined the cells, the molecular signals and the cellular scaffolds that are present in the wound-healing environment. We have identified a population of primary mesenchymal progenitor cells (MPCs) harvested from debrided human muscle tissue. These cells which are capable of differentiating down multiple pathways including bone and cartilage. MPCs have the potential to modulate differentiation due to their expression of multiple cytokines and growth factors. For example, they express TGFβ1, TGF 3, IL-10, GDF10 and BDNF at elevated levels compared to mesenchymal stem cells derived from human bone

marrow. Consistent with this data, tissue samples from traumatized muscle also display elevated TGFβ1, TGF 3, IL-10, and BDNF, compared to normal muscle. Given the capacity of MPCs to undergo osteogenesis and to express cytokines and growth factors, it is likely that these MPCs play a critical role in both fibrosis and HO formation. We have therefore used these MPCs as a platform onto which we hope to rationally generate a treatment strategy for HO. In addition, we have made use of a recently generated rat model for post-traumatic HO, which very closely mimics that seen in wounded veterans. We have combined these in vitro and in vivo approaches to identify a potential novel target for trauma-mediated muscle fibrosis that could block the formation of HO and potentially aid in muscle regeneration.

Heterotopic ossification (HO) is a frequent complication in battlefield injuries traumatized muscle as well as in the rehabilitation setting. Our study focuses on the investigation of the underlying molecular mechanisms of HO, which is essential for the identification of novel targeted therapies for the disease. For this purpose, we have developed an in vitro model for HO formation and progression consisting of Mesenchymal Progenitor Cells (MPCs) derived from high- and low-energy traumatized human muscle tissue (J Tissue Eng Regen Med. 2009;3(2):129-38) treated with the cytokine TGF-beta. MPCs are known for their ability to differentiate down multiple pathways including bone and cartilage, and as a result may play a role in the formation of HO. In addition, we previously reported that TGF-beta is up-regulated in traumatized muscle and its expression is localized to fibroproliferative lesions (J Orthop Res. 2011;29(10):1613-20), suggesting that activation of TGF-beta might play a role in the etiology of HO.

Since TGF-beta mediates most of the initial inflammatory and wound healing response in the traumatized muscle bed, we hypothesized that targeted inhibition of the TGF-beta pathway may be able to abrogate the unbalanced fibrotic phenotype and bone forming response observed in HO. To investigate that we analyzed the effects of treatment with the TGF-beta inhibitor drugs SB431542, LY2157299, Halofuginone and SIS3 in the expression levels of genes associated with early bone formation (CBFA1, also known as RUNX2) and fibrosis (FN1 and SERPINE1). For this experiment, MPCs from four independent donors were plated in 6-well plates at the density of 5,000 MPCs/cm2 and TGF-beta alone and the highest concentration of DMSO used to dilute the drugs were performed as treatment controls. Drug treatments were performed - in the presence of TGF-beta [10ng/ml] - as follows: SB431542 [0.3μM, 1μM and 3μM], LY2157299 [0.3μM, 1μM and 3μM], Halofuginone [3nM, 10nM and 30nM] and SIS3 [3μM, 10μM and 20μM]. Cells were treated for 48 hours and RNA samples were collected to investigate the treatments' effects on the expression profile of selected target genes.

As shown on Figures 1-2, MPCs were treated with TGF-beta alone had increased levels of the fibrotic markers FN1 (4.1-fold change) and SERPINE1 (5.6-fold change) compared to the vehicle control, while upon 48 hours of treatment with both classes of TGF-beta inhibitors the expression of the fibrotic markers was generally reduced (0.3- to 7.9-fold decrease) when compared to TGF-beta alone treated cells.

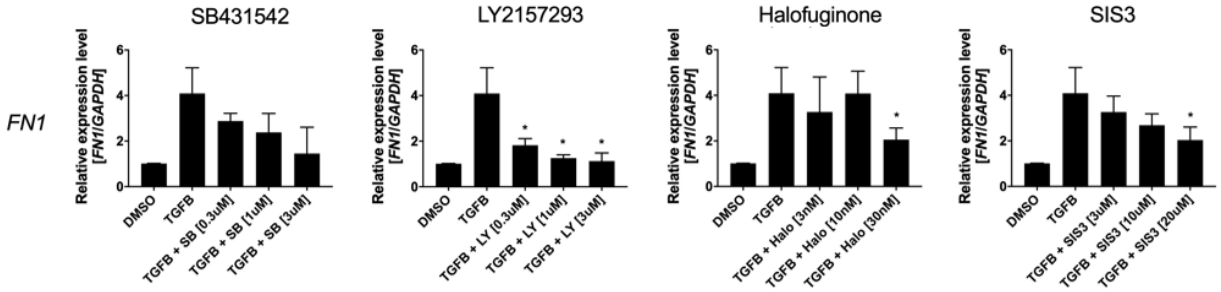

Figure 1 – Expression level of *FN1* upon treatment with SB431542, LY2157299, Halofuginone and SIS3 in the presence of TGF-beta [10ng/ml] treatment for 48 hours.

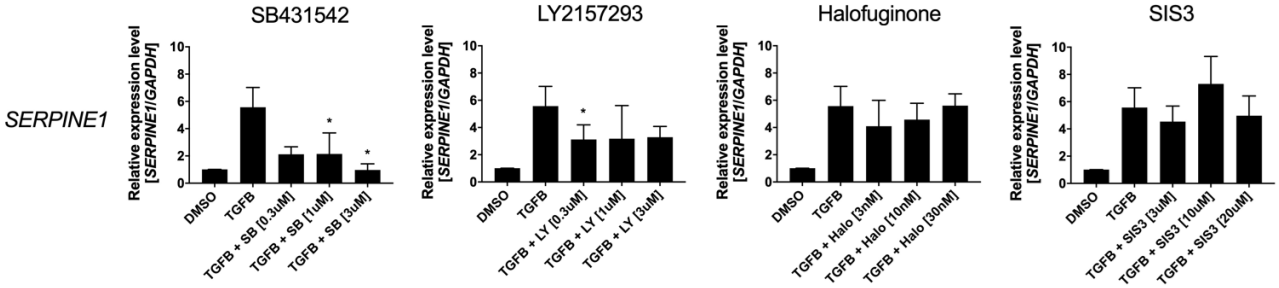

Figure 2 – Expression level of the *SERPINE1* upon treatment with SB431542, LY2157299, Halofuginone and SIS3 in the presence of TGF-beta [10ng/ml] treatment for 48 hours.

In addition, treatment of MPCs with TGF-beta alone for 48 hours showed increased expression of the osteogenesis regulator CBFA1 (1.9-fold change) compared to the vehicle control, while CBFA1 induction was moderately reversed (0.1- to 0.9-fold decrease) when treated with the TGF-beta inhibitors in the presence of TGF-beta (Figure 3).

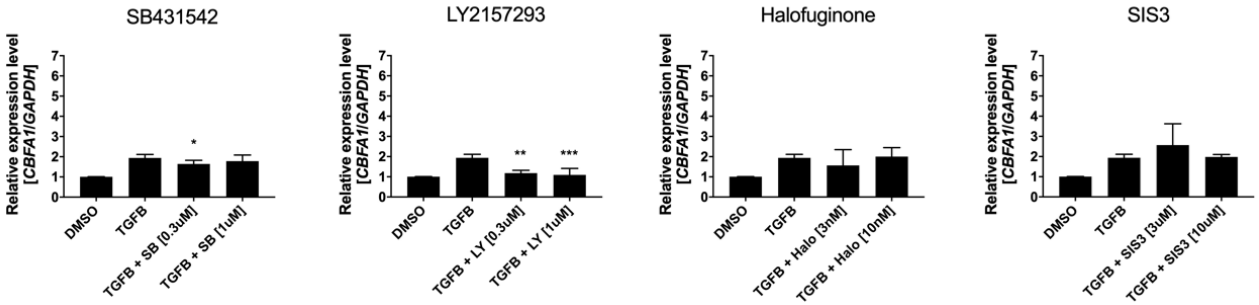

Figure 3 – Expression level of the *CBFA1* upon treatment with SB431542, LY2157299, Halofuginone and SIS3 in the presence of TGF-beta [10ng/ml] treatment for 48 hours.

Furthermore, to assess longer-term effects of the TGF-beta inhibitors, we performed additional experiments at an 8-days timepoint to assess the gene expression effects on CBFA1,

FN1 and SERPINE1 upon the drug treatments. Similarly, to the above-described experiments, TGF-beta alone and the highest concentration of DMSO used to dilute the drugs were performed as treatment controls. Drug treatments were performed - in the presence of TGF-beta [10ng/ml] - as follows: SB431542 [0.3μM and 1μM], LY2157299 [0.3μM and1μM], Halofuginone [3nM and 10nM] and SIS3 [3μM and 10μM]. Cells were treated for 8-days, with media and drugs refreshed on day 5, and RNA samples were collected to investigate the treatments' effects on the expression profile of the selected target genes.

As shown on Figures 4-5, MPCs were treated with TGF-beta alone had increased levels of the fibrotic markers FN1 (4.5-fold change) and SERPINE1 (7.2-fold change) compared to the vehicle control, while upon 8-days of treatment with both classes of TGF-beta inhibitors the expression of the fibrotic markers was mostly reduced (0.2- to 3.2-fold decrease) when compared to TGF-beta alone treated cells. Moreover, treatment of MPCs with TGF-beta alone for 8-days showed increased expression of the osteogenesis regulator CBFA1 (3.0-fold change) compared to the vehicle control, while CBFA1 induction was only moderately reversed (0.8- to 2.0-fold decrease) in three treatment conditions (Halofuginone 3nM, SIS3 3μM and SIS3 10μM), while it was increased in all other treatment conditions (1.1- to 3.8-fold increase) when treatments were performed in the presence of TGF-beta (Figure 6).

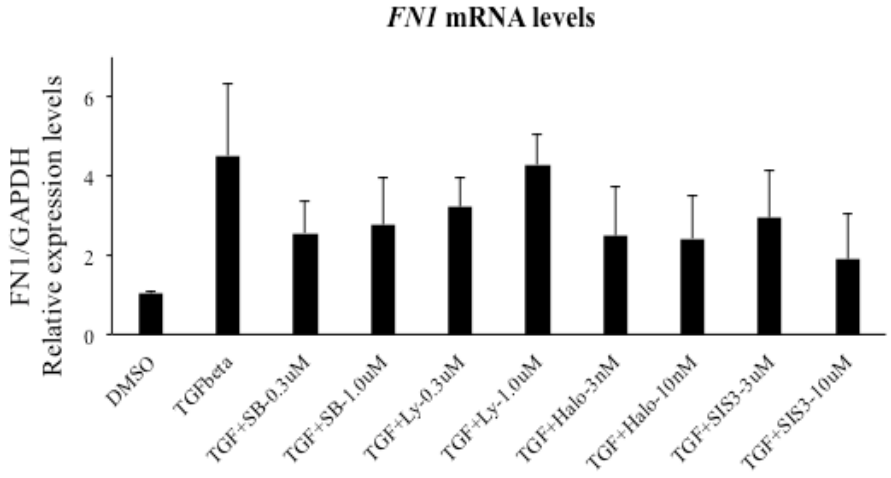

Figure 4 – Expression level of *FN1* upon treatment with SB431542, LY2157299, Halofuginone and SIS3 in the presence of TGF-beta [10ng/ml] treatment for 8-days.

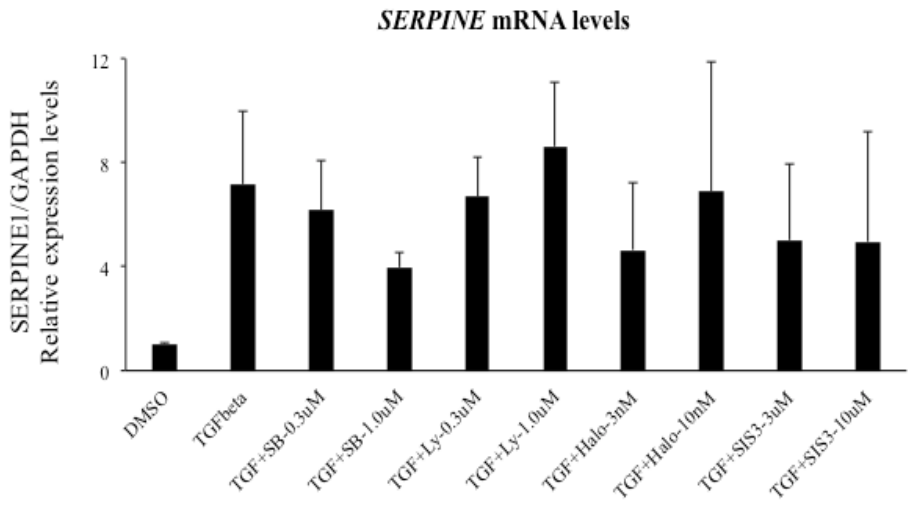

Figure 5 – Expression level of the *SERPINE1* upon treatment with SB431542, LY2157299, Halofuginone and SIS3 in the presence of TGF-beta [10ng/ml] treatment for 8-days.

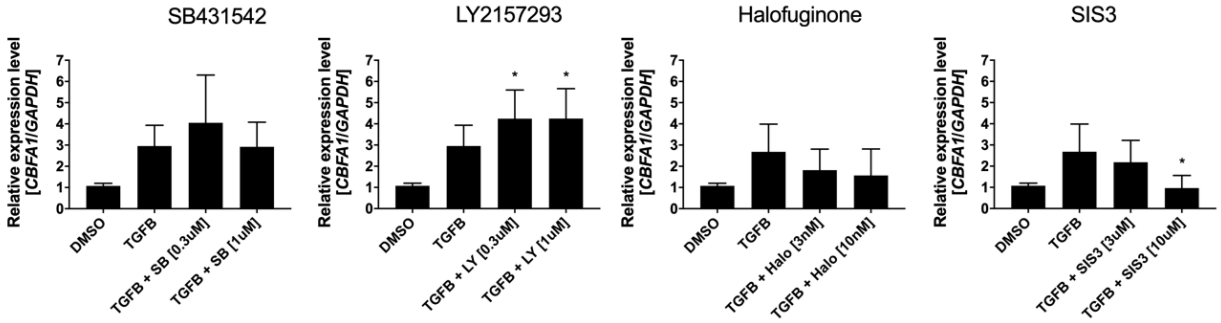

Figure 6 – Expression level of the *CBFA1* upon treatment with SB431542, LY2157299, Halofuginone and SIS3 in the presence of TGF-beta [10ng/ml] treatment for 8-days.

Following these findings, we focused our efforts to further investigate the effects of SB431542, LY2157299, Halofuginone and SIS3 treatments in the phosphorylation of SMAD2 and SMAD3 proteins. For these studies, we continued to use our in-vitro model for heterotopic ossification (HO) formation and progression that consists of primary human Mesenchymal Progenitor Cells (MPCs) derived from high- and low-energy traumatized muscle tissue (J Tissue Eng Regen Med. 2009;3(2):129-38) treated with TGF-beta. Initial experiments were performed with cells from two independent donors plated at 10-cm2 plates and seeded at 5,000 MPCs/cm2. TGF-beta alone and the highest concentration of DMSO used to dilute the drugs were performed as treatment controls. Drug treatments were performed - in the presence of TGF-beta [10ng/ml] - as follows: SB431542 [0.3μM, 1μM and 3μM], LY2157299 [0.3μM, 1μM and 3μM], Halofuginone [3nM, 10nM and 30nM] and SIS3 [3μM, 10μM and 20μM]. Cells were treated simultaneously with each inhibitor and TGF-beta for 30 minutes and protein samples were collected with RIPA buffer following manufacturer's instructions. Western blots were probed with antibodies against

phospho-SMAD2, phospho-SMAD3, total SMAD2, total SMAD3 and GAPDH following manufacture's recommendations for blocking and dilutions.

As shown on Figures 7-8, a dose response effect (inhibition) was observed on the phosphorylation of SMAD2 and SMAD3 upon treatment with both SB431542 and LY2157299 inhibitors. Importantly, the total levels of SMAD2 were not significantly changed (Figure 7), while the total levels of SMAD3 were moderately modulated in some conditions (Figure 8). In all cases, loading control was performed with GAPDH. Overall, these results confirm the effectiveness of the inhibitors SB431542 and LY2157299 to block the SMAD2/3 pathway in MPCs in vitro.

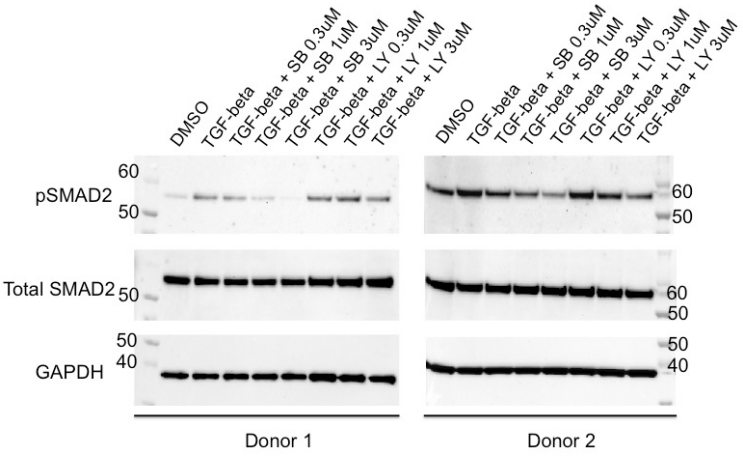

Figure 7 – Effects on the phosphorylation of SMAD2 (60KDa) and total SMAD2 (60KDa) upon treatment with SB431542 [0.3µM, 1µM and 3µM] and LY2157299 [0.3µM, 1µM and 3µM] in the presence of TGF-beta [10ng/ml] treatment for 30 minutes. Molecular weight is shown in Kilodalton. Loading control was performed with GAPDH. SB = SB431542; LY = LY2157299.

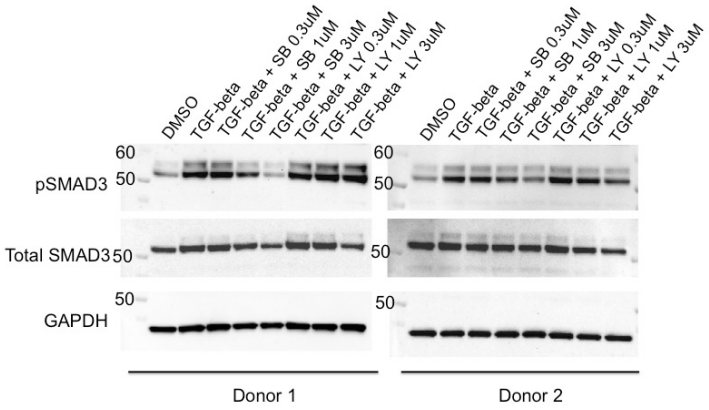

Figure 8 – Effects on the phosphorylation of SMAD3 (48-52 KDa) and total SMAD3 (48-52 KDa) upon treatment with SB431542 [0.3µM, 1µM and 3µM] and LY2157299 [0.3µM, 1µM and 3µM] in the presence of TGF-beta [10ng/ml] treatment for 30 minutes. Molecular weight is shown in Kilodalton. Loading control was performed with GAPDH. SB = SB431542; LY = LY2157299.

It has been previously reported that inhibition of phospho-SMAD3 by Halofuginone and SIS3 may happen upon pre-treatment of the cells with these inhibitors. In the literature, pre-treatments have varied from 1 to 24 hours, prior to stimulation with TGF-beta at variable concentrations. Since treatment with the inhibitors and TGF-beta simultaneously did not trigger the inhibition of phospho-SMAD3 (data shown in previous quarterly reports), we investigated different pre-treatment conditions and their effects on the phosphorylation of SMAD3.

For these studies, we continued to use our in-vitro model for heterotopic ossification (HO) formation and progression that consists of primary human MPCs derived from high- and low-energy traumatized muscle tissue (J Tissue Eng Regen Med. 2009;3(2):129-38) treated with TGF-beta. TGF-beta alone and the highest concentration of DMSO used to dilute the drugs were performed as treatment controls. Cells were pre-treated with each inhibitor at different concentrations and timepoints followed by TGF-beta treatment for 15 minutes, 30 minutes and/or 60 minutes. Protein samples were collected with RIPA buffer following manufacturer's instructions. Western blots were probed with antibodies against phospho-SMAD2, phospho-SMAD3, total SMAD2, total SMAD3 and GAPDH following manufacture's recommendations for blocking and dilutions.

Initially, pre-treatments were performed for 2h and 4h with Halofuginone [30nM] and SIS3 [20μM] followed by TGF-beta treatment for 30 minutes. As shown on Figure 9, no effects were observed on the phosphorylation of SMAD3 on these conditions.

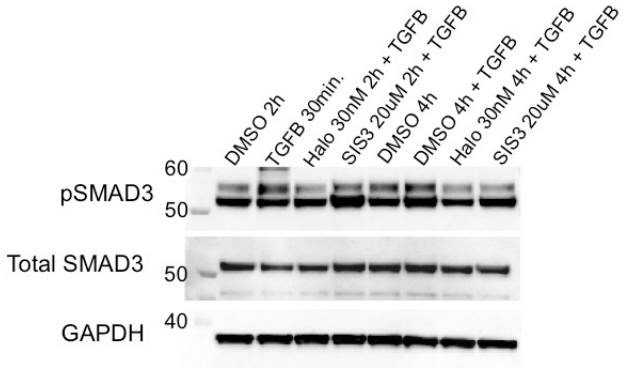

Figure 9 – Effects on the phosphorylation of SMAD3 (48-52 KDa) and total SMAD3 (48-52 KDa) upon 2h and 4h pre-treatment with Halofuginone [30nM] and SIS3 [20μM] followed by TGF-beta [10ng/ml] treatment for 30 minutes. Molecular weight is shown in Kilodaltons. Loading control was performed with GAPDH. Halo = Halofuginone.

Since no effects were observed with 2h and 4h pre-treatment, and the literature reports effects of SIS3 on the phosphorylation of SMAD3 after pre-treatments as long as 24h (Sci Rep. 2017;7(1):14530), we tested 24h pre-treatments of Halofuginone [30nM] and SIS3 [20μM] followed by TGF-beta [10ng/ml] treatment for 30 and 60 minutes. As shown on Figure 10, only Halofuginone [30nM] showed effects (inhibition/decrease) on the phosphorylation of SMAD3 after

both TGF-beta [10ng/ml] treatments for 30 and 60 minutes. Remarkably, the effects observed after 30 minutes of TGF-beta treatment were more robust than after 60 minutes of TGF-beta treatment, as a result the condition ‘Halofuginone [3nM, 10nM and 30nM] pre-treatment for 24h followed by TGF-beta [10ng/ml] treatment for 30 minutes’ was selected for the final dose response experiment (Figure 11). As expected, no effects were observed in phospho-SMAD2 and total SMAD2, while a dose-dependent response was observed on phospho-SMAD3, with some decrease observed on the levels of total SMAD3. Also, of importance, SIS3 [20μM] did not seem to present any effects on the phosphorylation of SMAD3 (Figure 10).

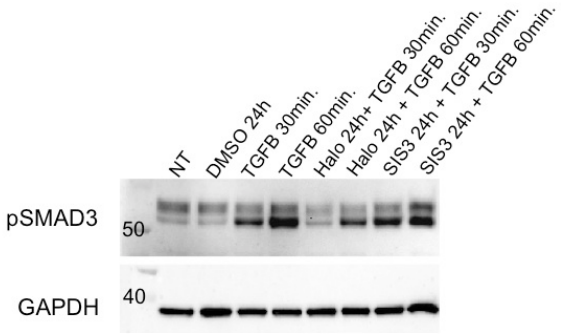

Figure 10 – Effects on the phosphorylation of SMAD3 (48-52 KDa) and upon 24h pre-treatment with Halofuginone [30nM] and SIS3 [20μM] followed by TGF-beta [10ng/ml] treatment for 30 and 60 minutes. Molecular weight is shown in Kilodaltons. Loading control was performed with GAPDH. Halo = Halofuginone.

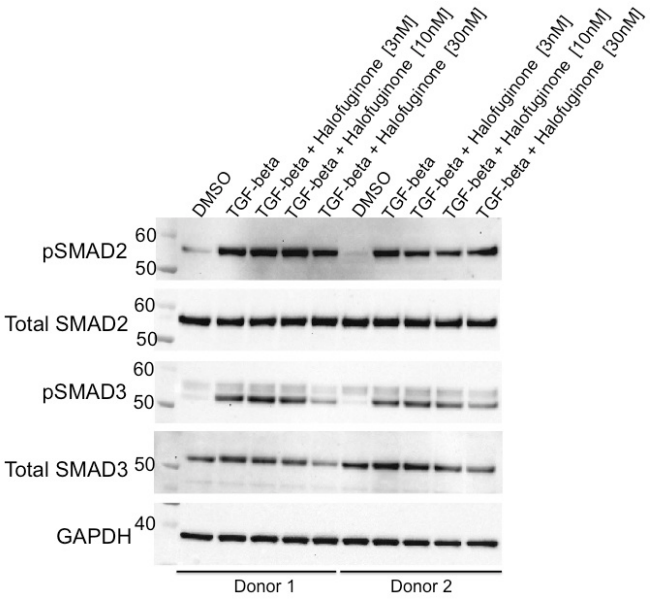

Figure 11 – Effects on the phosphorylation of SMAD2 (60KDa), total SMAD2 (60KDa), phosphorylation of SMAD3 (48-52 KDa) and total SMAD3 (48-52 KDa) upon treatment (24h pre-treatment) with Halofuginone [3nM, 10nM and 30nM] followed by TGF-beta [10ng/ml] treatment

for 30 minutes. Molecular weight is shown in Kilodaltons. Loading control was performed with GAPDH.

Upon these results, we contacted the company where we had purchased the drug SIS3 to inquire about the stability and half-life of the drug. The company suggested that multiple thaw-and-freeze cycles could possibly inactivate the drug. To test the hypothesis that the drug used in the above experiments was degraded or inactive, the company sent us a new batch of SIS3. As shown on Figure 12, this hypothesis was confirmed since with the new batch of SIS3 we observed decreased SMAD3 phosphorylation after treatment with SIS3 [20uM] for 12h and 24h followed by TGF-beta [10ng/ml] treatment for 30 minutes. Additionally, since the SIS3 pre-treatments for 12h and 24h demonstrated the best results regarding decreased phosphorylation of SMAD3, we performed SIS3 [20uM] pre-treatment for 12h and 24h followed by TGF-beta [10ng/ml] treatment for 15 and 30 minutes. As shown on Figure 13, the results (decrease/inhibition in the phosphorylation of SMAD3) obtained with SIS3 treatment followed by TGF-beta [10ng/ml] treatment for 15 minutes were more robust compared to the TGF-beta treatment for 30 minutes. Of note, we also purchased SIS3 from another brand and observed similar results.

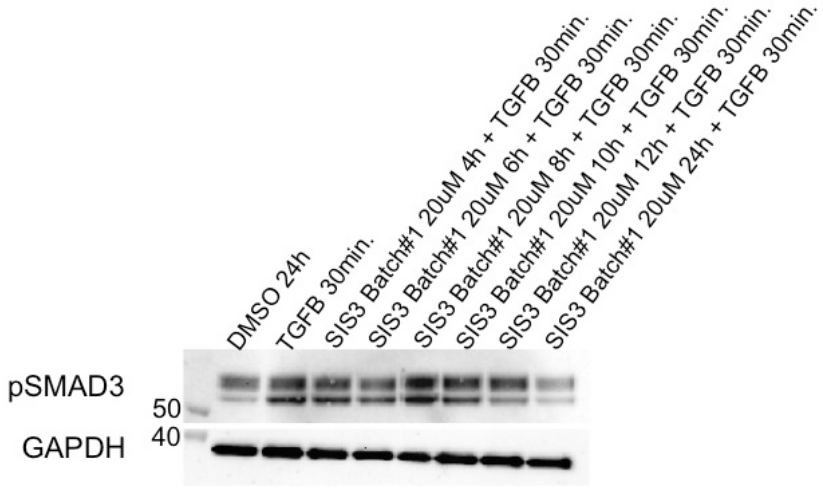

Figure 12 – Effects on the phosphorylation of SMAD3 (48-52 KDa) and upon pre-treatment for 4h, 6h, 8h, 10h, 12h and 24h with SIS3 [20μM] followed by TGF-beta [10ng/ml] treatment for 30 minutes. Molecular weight is shown in Kilodaltons. Loading control was performed with GAPDH.

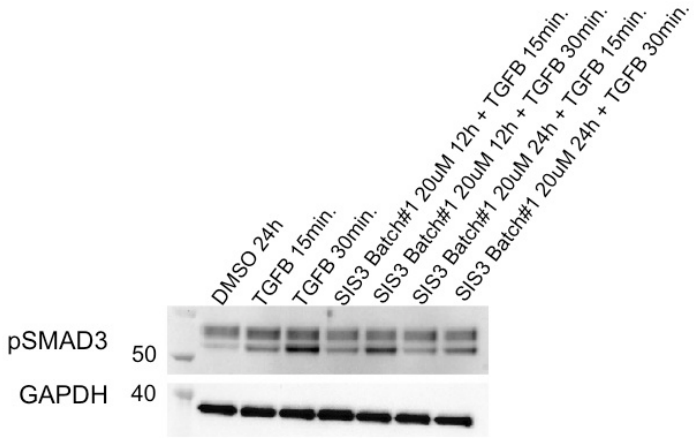

Figure 13 – Effects on the phosphorylation of SMAD3 (48-52 KDa) and upon pre-treatment for 12h and 24h with SIS3 [20μM] followed by TGF-beta [10ng/ml] treatment for 15 and 30 minutes. Molecular weight is shown in Kilodaltons. Loading control was performed with GAPDH.

As a result, the condition 'SIS3 [5μM, 10μM and 20μM] pre-treatment for 24h followed by TGF-beta [10ng/ml] treatment for 15 minutes' was selected for the final dose response experiment (Figure 14). In these conditions, we observed no effects in phospho-SMAD2 and total SMAD2, a dose-dependent response on phospho-SMAD3, while some decrease was also observed on the levels of total SMAD3.

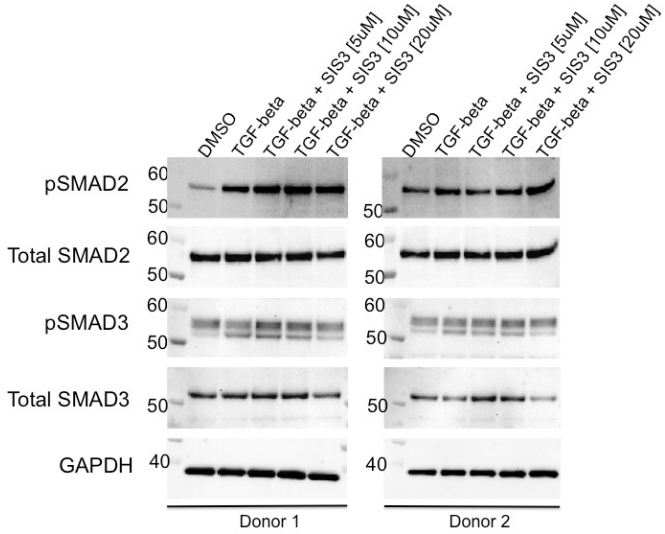

Figure 14 – Effects on the phosphorylation of SMAD2 (60KDa), total SMAD2 (60KDa), phosphorylation of SMAD3 (48-52 KDa) and total SMAD3 (48-52 KDa) upon 24h pre-treatment with SIS3 [5μM, 10μM and 20μM] followed by TGF-beta [10ng/ml] treatment for 15 minutes. Molecular weight is shown in Kilodaltons. Loading control was performed with GAPDH.

Following these Western blot studies, we focused our efforts to investigate the potential for the TGF-beta targeted therapies to inhibit the formation of fibrotic nodules. Since fibrosis appears to play a central role in HO development and progression, we pursued the development of an in vitro model of fibrotic nodule formation using human primary human MPCs derived from high- and low-energy traumatized muscle tissue (J Tissue Eng Regen Med. 2009;3(2):129-38) treated with TGF-beta. An important aspect of this model is that it is mediated by TGF-beta, an inflammatory factor understood to drive the fibrotic response. This model relies on the plating of cells on poly-L-lysine coated dishes, which are then subsequently treated with TGF-beta (Am J Physiol Renal Physiol. 2007;293(2):F631-40). In the absence of TGF-beta, the cells remain in a monolayer and when treated with TGF-beta, the cells migrate into spherical nodules within 48-96 hours. The cells strongly adhere to each other and form a multicellular 3-dimensional nodule which is quite stable over days in culture. In addition, these nodules are remarkably similar to those observed in traumatized muscle tissue (preliminary data, not shown).

Initial studies were performed with poly-L-lysine pre-coated 6-well plates treated with TGF-beta [10 ng/mL] alone or in combination with DMSO or ALK5 inhibitors (SB431542 and LY2157299) for 4- and 6-days. Interestingly, even though cell movement was observed, as evidenced by the existence of space in the monolayer of cells, no fibrotic nodules were observed (Figure 15).

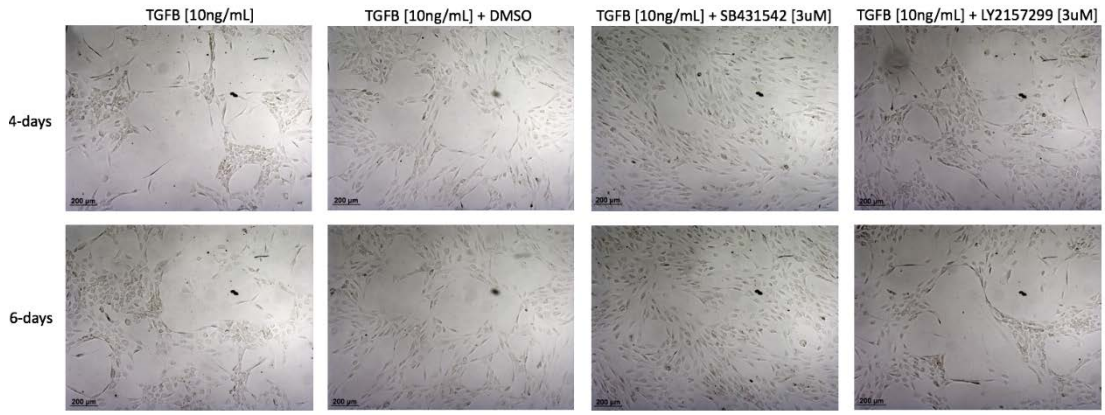

Figure 15 – MPCs cultured on poly-L Lysine pre-coated 6-well plates and treated with TGF-beta [10 ng/mL] alone or in combination with DMSO, SB431542 [3 uM] or LY2157299 [3 uM] for 4- and 6-days. TGFB = TGF-beta.

Next, to examine the possibility that the concentration of TGF-beta needed to be increased, we performed a similar experiment as described above, and tested two concentrations of TGF-beta [10 ng/mL] and [20 ng/mL] for 6-days. In addition, we tested a new dilution of TGF-beta compared to the previously diluted solution of TGF-beta used above. As observed on Figure 16, cell movement was observed, but no fibrotic nodules were formed (Figure 16). Of note, more cell movement was observed with the new dilution of TGF-beta – independent of the concentration – suggesting that the new dilution was more effective than the older dilution. As a

result, the older TGF-beta dilution was discarded and additional experiments were exclusively performed with the new dilution.

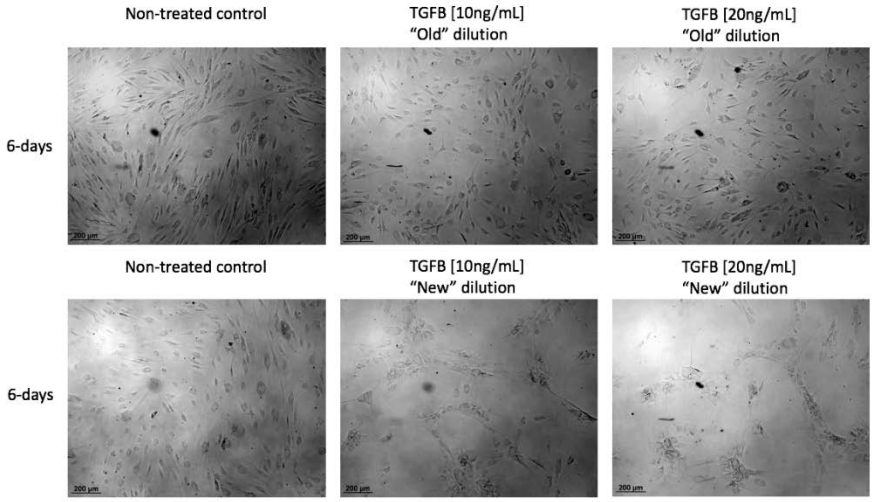

Figure 16 – MPCs cultured on poly-L Lysine pre-coated 6-well plates and treated with two dilutions of TGF-beta [10 ng/mL] or [20 ng/mL]. Previously diluted TGF-beta is identified as "old" dilution and freshly diluted TGF-beta is identified as "new" dilution. Treatments were performed for 6-days. TGFB = TGF-beta.

As a result of these preliminary data, we hypothesized that the surface well area of a 6-wells plate (9.6 cm^2) is too large, and upon 80-90% confluence comprised of too many cells to favor the formation of the fibrotic nodules. To investigate this hypothesis, we performed the next experiment in a 96-well plate coated by hand with poly-L-lysine seeded with 10,000 MPCs per well. Of note, the surface area of one well of a 96-well plate is 0.32 cm^2. Treatments were performed in the presence of TGF-beta [10 ng/mL], with the exception of non-treated and DMSO controls. Each condition was performed in triplicate, and the total number of nodules in each well from each condition were counted and averaged after 4-days of treatment.

As showed on Figure 17, non-treated and DMSO controls continued to proliferate in a monolayer of cells. In addition, TGF-beta [10 ng/mL] alone formed fibrotic nodules, validating the experimental conditions. In the presence of the ALK5 inhibitors (SB431542 and LY2157299) no nodules were observed. Interestingly, in the presence of the SMAD3 inhibitor Halofuginone, fibrotic nodules were observed to a similar extent as the TGF-beta control. Finally, in the presence of the SMAD3 inhibitor SIS3, a reduction in the number of nodules was clearly observed (Figure 17).

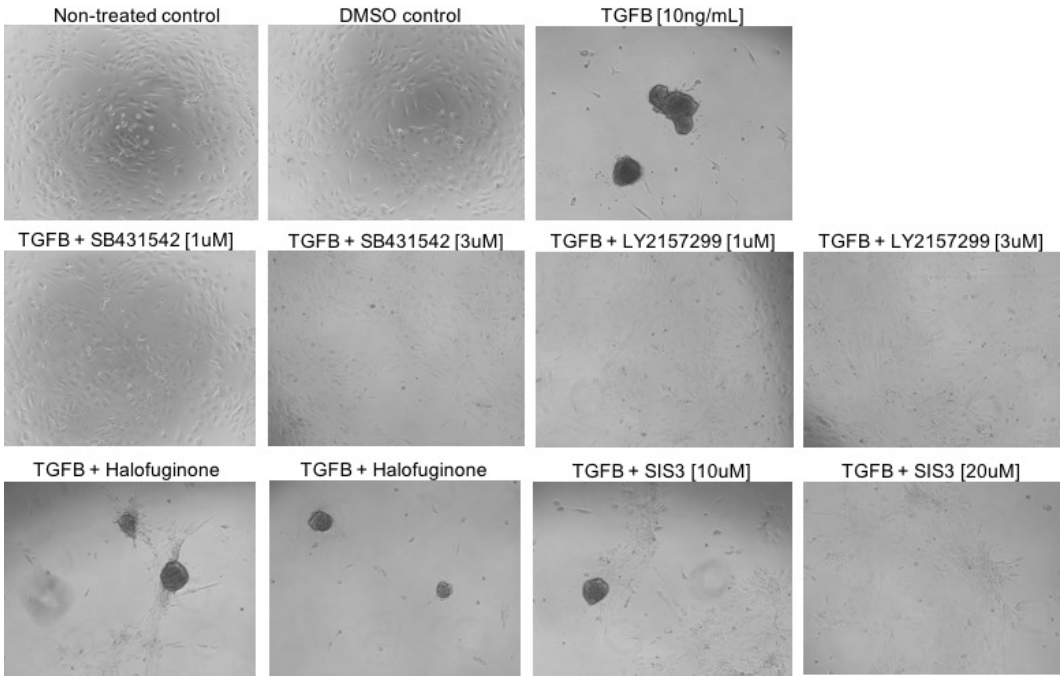

Figure 17 – MPCs cultured on poly-L lysine coated 96-well plates and treated with TGF-beta [10 ng/mL] alone (control), TGF-beta [10 ng/mL] + SB431542 [1uM and 3uM], TGF-beta [10 ng/mL] + LY2157299 [1uM and 3uM], TGF-beta [10 ng/mL] + Halofuginone [10nM and 30nM] and TGF-beta [10 ng/mL] + SIS3 [10uM and 20uM]. Non-treated cells and DMSO treated cells were used as controls. Treatments were performed for 4-days. TGFB = TGF-beta.

In total, this experiment was performed with three independent donors, and the number of nodules' individual averages of each donor (average of the triplicate wells, Figure 18) as well as the average of the donors combined (Figure 19) are shown. Statistical analysis was performed with Student's t-test. Altogether, these experiments clearly demonstrated that SB431542, LY2157299 and SIS3 significantly inhibited nodule formation induced by the TGF-beta treatment.

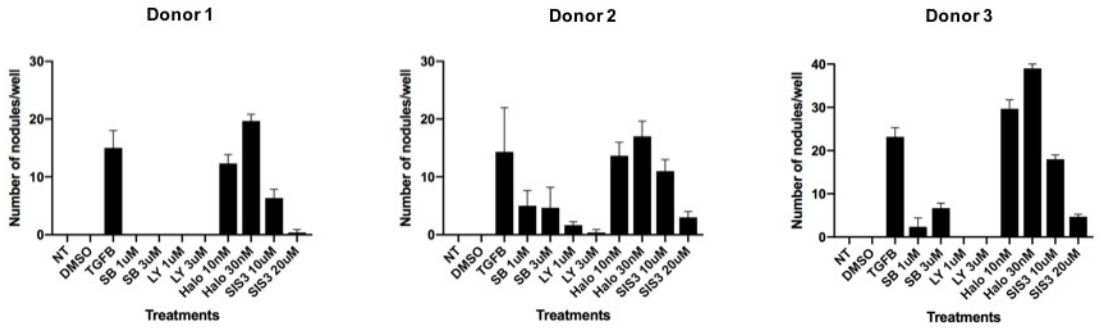

Figure 18 – Number of nodules from each individual donor (average of triplicate wells) following treatment with TGF-beta [10 ng/mL] alone (control), TGF-beta [10 ng/mL] + SB431542 [1uM and 3uM], TGF-beta [10 ng/mL] + LY2157299 [1uM and 3uM], TGF-beta [10 ng/mL] + Halofuginone [10nM and 30nM] and TGF-beta [10 ng/mL] + SIS3 [10uM and 20uM] for 4-days]. Non-treated cells and DMSO treated cells were used as controls.

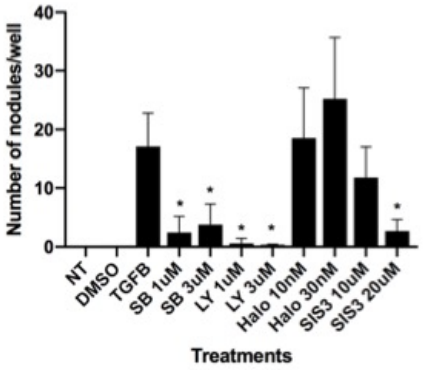

Figure 19 – Number of nodules from each individual treatment (average of three independent donors) following treatment with TGF-beta [10 ng/mL] alone (control), TGF-beta [10 ng/mL] + SB431542 [1uM and 3uM], TGF-beta [10 ng/mL] + LY2157299 [1uM and 3uM], TGF-beta [10 ng/mL] + Halofuginone [10nM and 30nM] and TGF-beta [10 ng/mL] + SIS3 [10uM and 20uM] for 4-days]. Non-treated cells and DMSO treated cells were used as controls. Statistical analysis was performed with Student's t-test. *$p<0.05$.

Following these findings, we focused our efforts to (i) induce osteogenic differentiation following fibrotic nodule formation and (ii) investigate the gene expression profile of fibrotic markers following the formation of fibrotic nodules *in vitro*. Our initial efforts focused on inducing osteogenic differentiation following the fibrotic nodule formation to asses if the fibrotic nodules have the ability to undergo osteogenic induction (similar to MPCs when cultured in monolayer conditions), and if treatment with the TGF-beta inhibitors would have any effect on the osteogenic induction. Osteogenic differentiation was performed as previously described (J Bone Joint Surg Am. 2008;90(11):2390-8, PLoS One. 2014;9(12):e114318), followed by 2% Alizarin Red S at pH 4.2 for evidence of a mineralized matrix. Briefly, monolayer cultures of MPCs were seeded at a density of 5,000 cells/cm^2 and treated for 2-, 4- or 5-weeks with osteogenic medium, consisting

of Dulbecco's Modified Eagle Medium with 10% fetal bovine serum supplemented with10 mM β-Glycerol phosphate, 50 μg/mL ascorbic acid, 10 nM 1,25-di-hydroxyvitamin D3 and 0.01 μM dexamethasone.

As shown on two independent donors (Figures 20-21), after 5-weeks in osteoinductive medium, we observed histological evidence of increased matrix mineralization by Alizarin red staining. However, no differences were observed between the treatments. Interestingly, shorter times in osteoinductive medium (2- and 4-weeks, Figures 22 and 23, respectively) did not demonstrate any differences in the increase of matrix mineralization by Alizarin red staining.

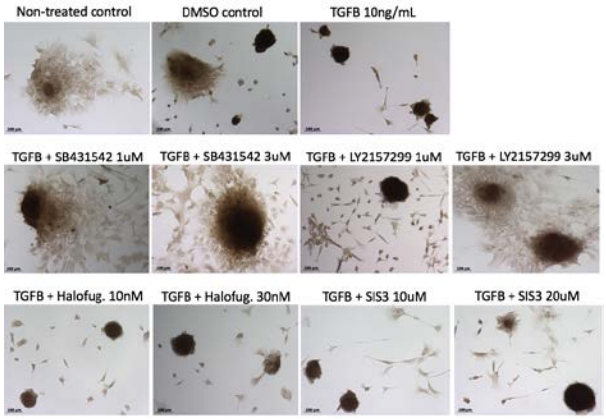

Figure 20 – Osteogenic differentiation (5-weeks, Donor 1) following the fibrotic nodule formation assay. MPCs (Donor 1) cultured on poly-L lysine coated 96-well plates and treated with TGF-beta [10 ng/mL] alone (control), TGF-beta [10 ng/mL] + SB431542 [1uM and 3uM], TGF-beta [10 ng/mL] + LY2157299 [1uM and 3uM], TGF-beta [10 ng/mL] + Halofuginone [10nM and 30nM] and TGF-beta [10 ng/mL] + SIS3 [10uM and 20uM] for 4-days followed by osteogenic induction for 5-weeks. Non-treated cells and DMSO treated cells were used as treatment controls. TGFB = TGF-beta, Halofug. = Halofuginone. 10X magnification.

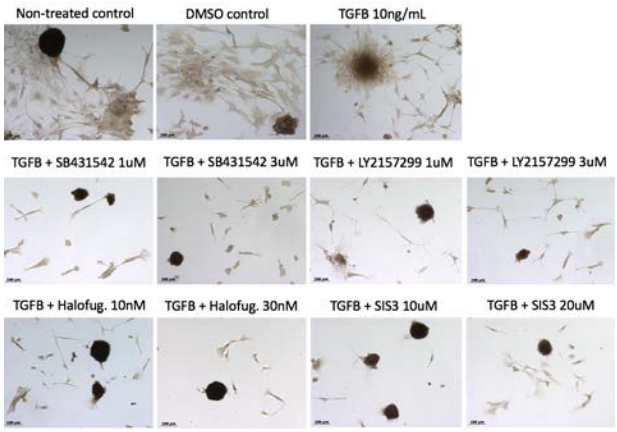

Figure 21 – Osteogenic differentiation (5-weeks, Donor 2) following the fibrotic nodule formation assay. MPCs cultured on poly-L lysine coated 96-well plates and treated with TGF-beta [10 ng/mL] alone (control), TGF-beta [10 ng/mL] + SB431542 [1uM and 3uM], TGF-beta [10 ng/mL]

+ LY2157299 [1uM and 3uM], TGF-beta [10 ng/mL] + Halofuginone [10nM and 30nM] and TGF-beta [10 ng/mL] + SIS3 [10uM and 20uM] for 4-days followed by osteogenic induction for 5-weeks. Non-treated cells and DMSO treated cells were used as treatment controls. TGFB = TGF-beta, Halofug. = Halofuginone. 10X magnification.

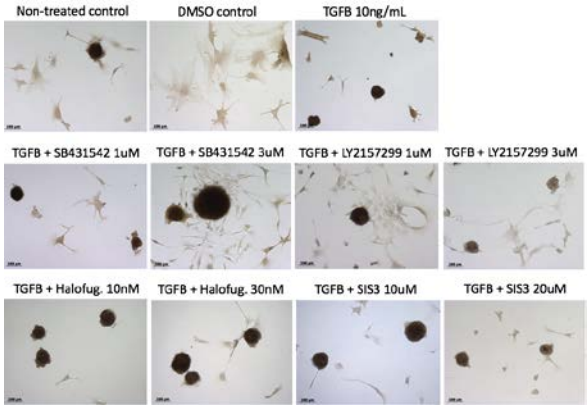

Figure 22 – Osteogenic differentiation (2-weeks) following the fibrotic nodule formation assay. MPCs cultured on poly-L lysine coated 96-well plates and treated with TGF-beta [10 ng/mL] alone (control), TGF-beta [10 ng/mL] + SB431542 [1uM and 3uM], TGF-beta [10 ng/mL] + LY2157299 [1uM and 3uM], TGF-beta [10 ng/mL] + Halofuginone [10nM and 30nM] and TGF-beta [10 ng/mL] + SIS3 [10uM and 20uM] for 4-days followed by osteogenic induction for 2-weeks. Non-treated cells and DMSO treated cells were used as treatment controls. TGFB = TGF-beta, Halofug. = Halofuginone. 10X magnification.

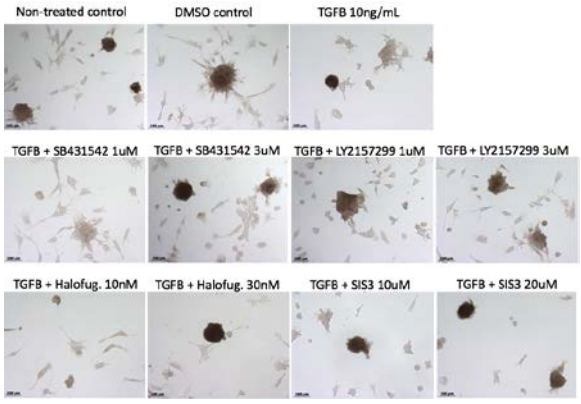

Figure 23 – Osteogenic differentiation (4-weeks) following the fibrotic nodule formation assay. MPCs cultured on poly-L lysine coated 96-well plates and treated with TGF-beta [10 ng/mL] alone (control), TGF-beta [10 ng/mL] + SB431542 [1uM and 3uM], TGF-beta [10 ng/mL] + LY2157299 [1uM and 3uM], TGF-beta [10 ng/mL] + Halofuginone [10nM and 30nM] and TGF-beta [10 ng/mL] + SIS3 [10uM and 20uM] for 4-days followed by osteogenic induction for 4-weeks. Non-treated cells and DMSO treated cells were used as treatment controls. TGFB = TGF-beta, Halofug. = Halofuginone. 10X magnification.

In addition to the osteogenic induction, we are focusing on the investigation of the gene expression profile of fibrotic markers following the formation of fibrotic nodules *in vitro*. To investigate that we collected RNA and performed quantitative PCR analyses for target genes following the 4-days of the fibrotic nodules' formation assay. In accordance to our previously shown data on the total number of fibrotic nodules formed with this assay, the expression of the fibrotic markers *COL1A1*, *FN1* and *SERPINE1* are strongly down-regulated (Figures 24-25) upon treatment with the ALK5 inhibitors (SB431542 and LY2157299) and up-regulated or equivalent to the TGF-beta control upon treatment with the SMAD inhibitors (Halofuginone and SIS3). Interestingly, the fibrotic marker *ACTA2* is also down-regulated upon treatment with the ALK5 inhibitors and mostly equivalent or decreased (Halofuginone [30nM]) to the TGF-beta control upon treatment with the SMAD inhibitors (Figures 24-25).

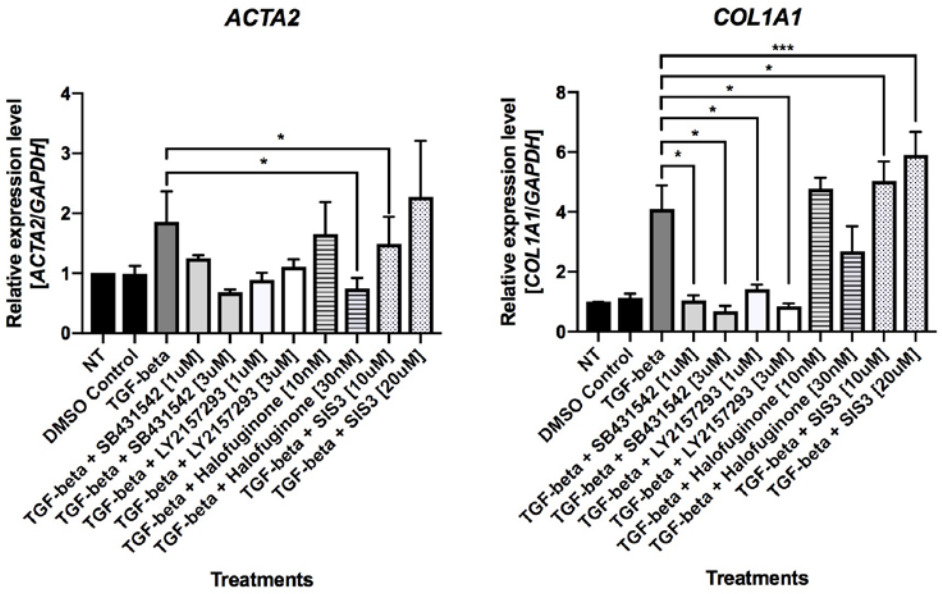

Figure 24 – Quantitative PCR analysis of the fibrotic markers *ACTA2* and *COL1A1* following the fibrotic nodule formation assay. MPCs were cultured on poly-L lysine coated 96-well plates and treated with TGF-beta [10 ng/mL] alone (control), TGF-beta [10 ng/mL] + SB431542 [1uM and 3uM], TGF-beta [10 ng/mL] + LY2157299 [1uM and 3uM], TGF-beta [10 ng/mL] + Halofuginone [10nM and 30nM] and TGF-beta [10 ng/mL] + SIS3 [10uM and 20uM] for 4-days followed by RNA extraction and qPCR analysis. *p<0.05, *** p≦0.001, T-test 1-tail.

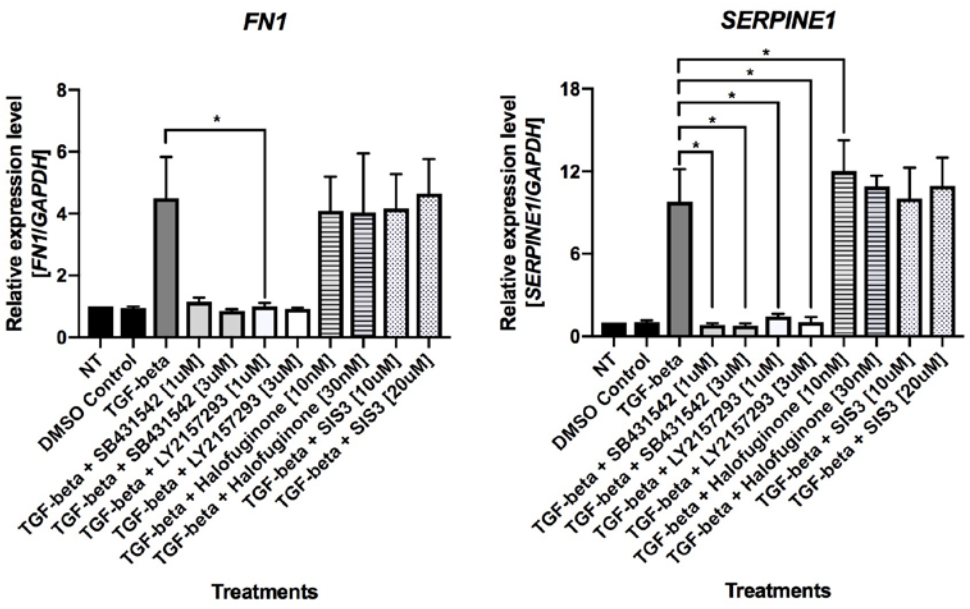

Figure 25 – Quantitative PCR analysis of the fibrotic markers *FN1* and *SERPINE1* following the fibrotic nodule formation assay. MPCs were cultured on poly-L lysine coated 96-well plates and treated with TGF-beta [10 ng/mL] alone (control), TGF-beta [10 ng/mL] + SB431542 [1uM and 3uM], TGF-beta [10 ng/mL] + LY2157299 [1uM and 3uM], TGF-beta [10 ng/mL] + Halofuginone [10nM and 30nM] and TGF-beta [10 ng/mL] + SIS3 [10uM and 20uM] for 4-days followed by RNA extraction and qPCR analysis. *p<0.05, T-test 1-tail.

We also investigated the expression of the osteogenic markers *CBFA1*, *ALP* and *Osteocalcin* on these samples (following the formation of fibrotic nodules *in vitro*). As shown on Figure 26, *CBFA1* was significantly down-regulated upon treatment with the ALK5 inhibitors (SB431542 and LY2157299) and moderately up-regulated - but not statistically significant - upon treatment with the SMAD inhibitors (Halofuginone and SIS3). Interestingly, *ALP* was decreased upon treatment with TGF-beta alone, up-regulated upon treatment with the ALK5 inhibitors (compared to TGF-beta alone) and down-regulated or unchanged upon treatment with the SMAD inhibitors (compared to TGF-beta alone). Finally, *Osteocalcin* was slightly up-regulated upon treatment with ALK5 inhibitors and SIS3 at the higher concentration, while all the other treatment conditions remained unchanged.

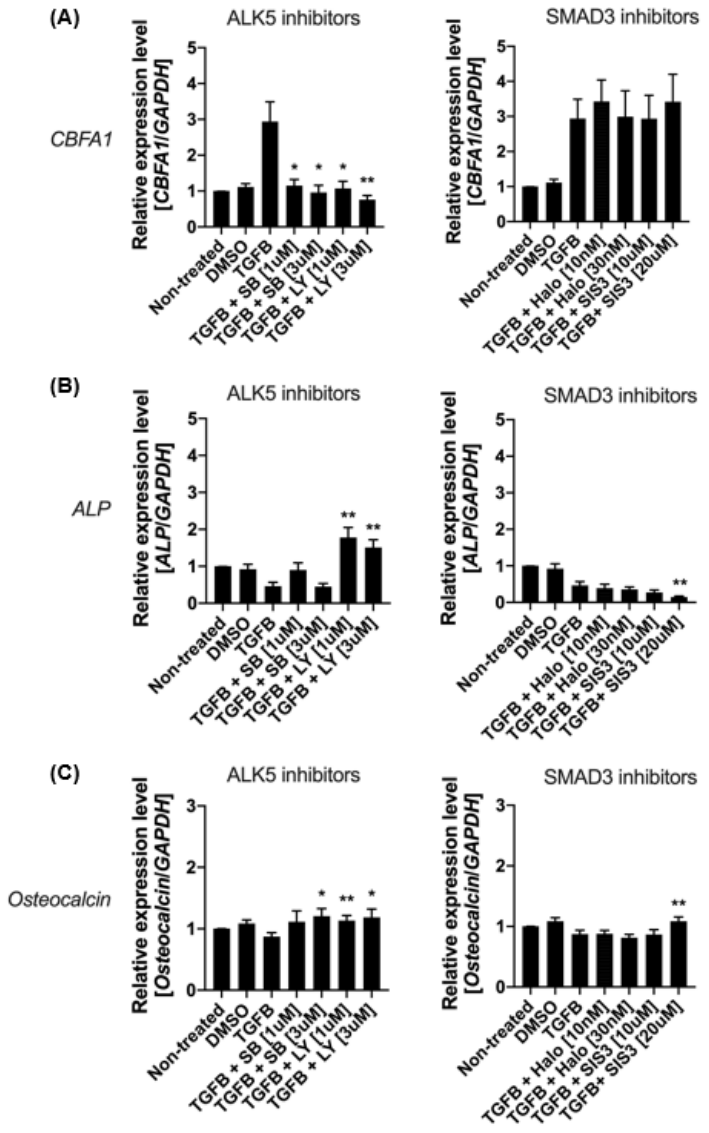

Figure 26 – Quantitative PCR analysis of the osteogenic markers *CBFA1*, *ALP* and *Osteocalcin* following the fibrotic nodule formation assay. MPCs were cultured on Poly-L-Lysine coated 96-well plates and treated with TGF-beta [10 ng/mL] alone (control), TGF-beta [10 ng/mL] + SB431542 [1uM and 3uM], TGF-beta [10 ng/mL] + LY2157299 [1uM and 3uM], TGF-beta [10 ng/mL] + Halofuginone [10nM and 30nM] and TGF-beta [10 ng/mL] + SIS3 [10uM and 20uM] for 4-days followed by RNA extraction and qPCR analysis. DMSO alone was used as vehicle control. *p<0.05, **p≦0.01, *** p≦0.001, T-test 1-tail.

In addition, we chose to perform a comparison between the gene expression profile of the fibrotic and osteogenic markers following the formation of fibrotic nodules *in vitro* and following MPCs cultured and treated with TGF-beta inhibitors in a 3-dimensional nanofiber plate. The aim of this comparison was to investigate if the type of 3-dimensional system where the cells are cultured has an impact on the response to the TGF-beta inhibitors as assessed by the mRNA

expression of fibrotic and osteogenic markers. To investigate that we collected RNA and performed quantitative PCR analyses for fibrotic and osteogenic target genes following 4-days of treatment with the TGF-beta inhibitors when the MPCs where cultured in commercially available nanofiber plates. As shown on Figure 27, the commercial nanofiber plate used on these experiments has fibers on a random orientation, which we believe mimics the fibers formed on the fibrotic/scar tissue following a traumatic injury *in vivo*.

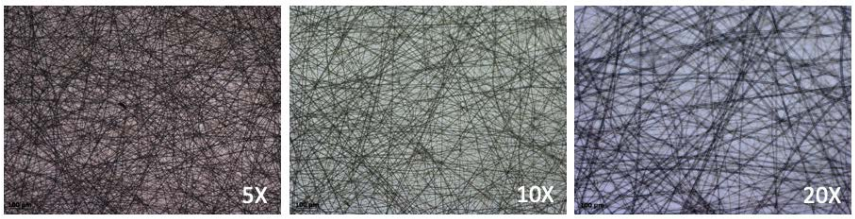

Figure 27 – Commercial nanofiber plate displays randomly orientated fibers. Different magnifications are indicated in each panel.

Following treatment with the TGF-beta inhibitors, the MPCs cultured on the nanofiber plates demonstrated mostly a down-regulated expression of the fibrotic markers *ACTA2*, *COL1A1*, *FN1* and *CDH2*, with the exception of the cells treated with Halofuginone [30nM], where the levels of *CDH2* were up-regulated (Figures 28-29). In addition, *SERPINE1*, *VIMENTIN* and *MMP2* were mostly unchanged, again with the exception of the cells treated with Halofuginone [30nM], where the levels of *SERPINE1* were robustly up-regulated and the levels of *MMP2* were robustly down-regulated. Finally, *MMP9* levels were unchanged on cells treated with SB431542 [3uM] and down-regulated on cells treated with LY2157299 [3uM], Halofuginone [30nM] and SIS3 [20uM], with the less robust effect observed upon the SIS3 [20uM] treatment.

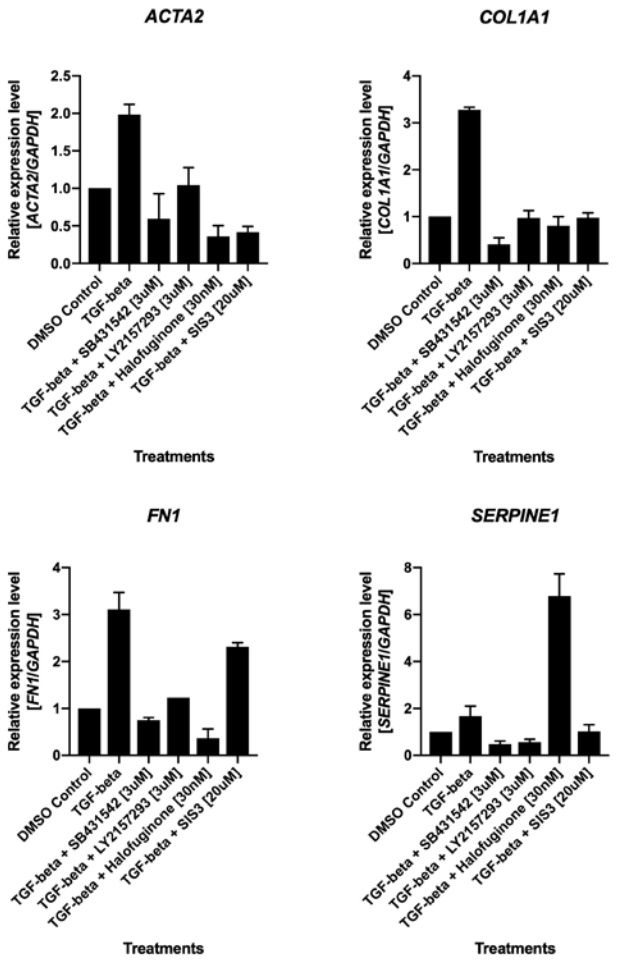

Figure 28 – Quantitative PCR analysis of the fibrotic markers *ACTA2*, *COL1A1, FN1* and *SERPINE1*. MPCs were cultured on randomly oriented nanofiber plates and treated with TGF-beta [10 ng/mL] alone (control), TGF-beta [10 ng/mL] + SB431542 [3uM], TGF-beta [10 ng/mL] + LY2157299 [3uM], TGF-beta [10 ng/mL] + Halofuginone [30nM] and TGF-beta [10 ng/mL] + SIS3 [20uM] for 4-days followed by RNA extraction and qPCR analysis. DMSO alone was used as vehicle control. Results represent the average of two independent donors.

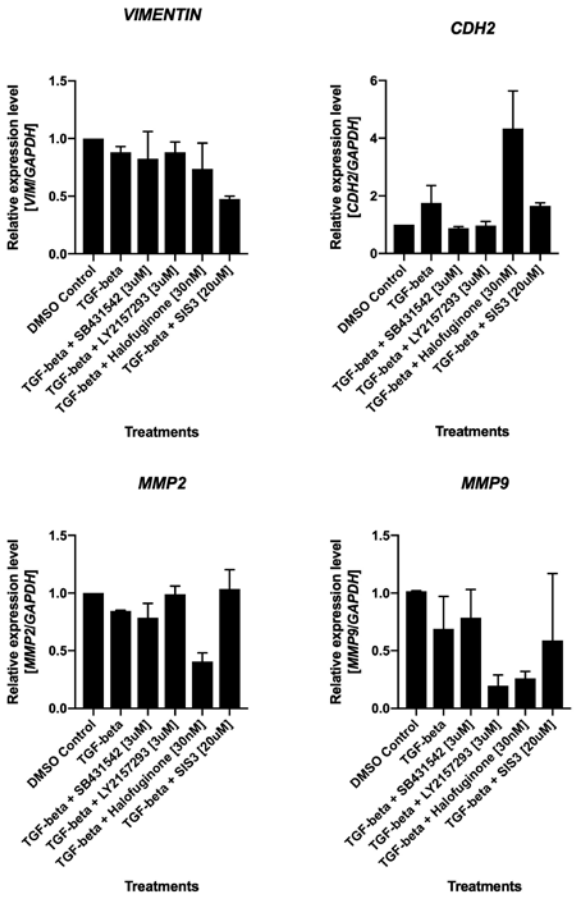

Figure 29 – Quantitative PCR analysis of the fibrotic markers *VIMENTIN*, *CDH2, MMP2* and *MMP9*. MPCs were cultured on randomly oriented nanofiber plates and treated with TGF-beta [10 ng/mL] alone (control), TGF-beta [10 ng/mL] + SB431542 [3uM], TGF-beta [10 ng/mL] + LY2157299 [3uM], TGF-beta [10 ng/mL] + Halofuginone [30nM] and TGF-beta [10 ng/mL] + SIS3 [20uM] for 4-days followed by RNA extraction and qPCR analysis. DMSO alone was used as vehicle control. Results represent the average of two independent donors.

Interestingly, following treatment with the TGF-beta inhibitors, the MPCs cultured on the nanofiber plates demonstrated no significant changes on the expression levels of *CBFA1*, while treatment with the TGF-beta inhibitors consistently down-regulated the expression levels of *ALP* (Figure 30). Lastly, the levels of *Osteocalcin* were mostly unchanged, with the exception of the cells treated with SB431542 [3uM], which demonstrated increased expression of *Osteocalcin* mRNA levels (Figure 30).

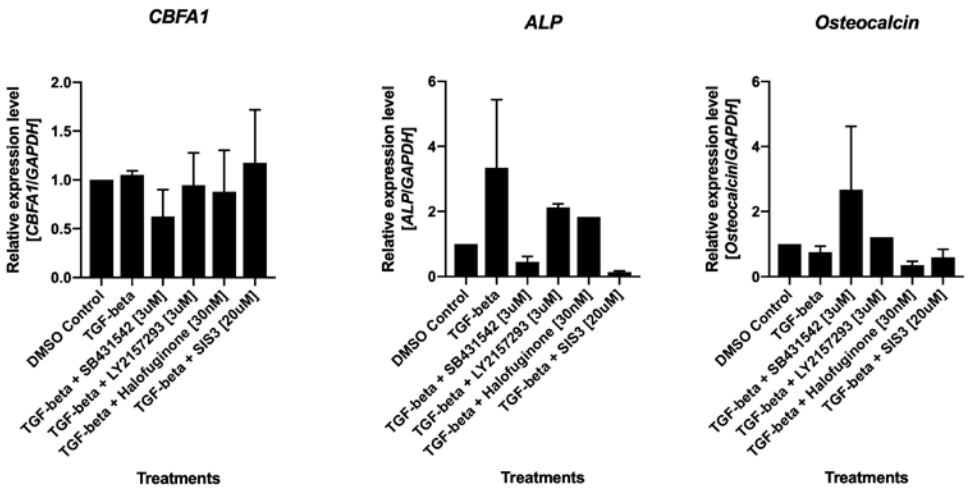

Figure 30 – Quantitative PCR analysis of the osteogenic markers *CBFA1*, *ALP* and *Osteocalcin*. MPCs were cultured on randomly oriented nanofiber plates and treated with TGF-beta [10 ng/mL] alone (control), TGF-beta [10 ng/mL] + SB431542 [3uM], TGF-beta [10 ng/mL] + LY2157299 [3uM], TGF-beta [10 ng/mL] + Halofuginone [30nM] and TGF-beta [10 ng/mL] + SIS3 [20uM] for 4-days followed by RNA extraction and qPCR analysis. DMSO alone was used as vehicle control. Results represent the average of two independent donors.

We also continued to focus our efforts to investigate the ability of the fibrotic nodules to undergo osteogenic differentiation following the formation of fibrotic nodules *in vitro*. Following the fibrotic nodules formation *in vitro*, cells (nodules) were induced to osteogenic differentiation for 4-weeks with an *in-house* previously reported osteogenic media (J Bone Joint Surg Am. 2008;90(11):2390-8) and commercially available osteogenic media. A control plate were cells grew in a monolayer condition was cultured at the same time with the same two osteogenic media and general media (non-osteogenic condition). Osteogenic differentiation was confirmed by Alizarin Red staining following a previously published protocol (J Bone Joint Surg Am. 2008;90(11):2390-8). As shown on Figure 31 A-B, both osteogenic media conditions induced cells to osteogenic differentiation on the control plate, however, the commercial media did appear to be more efficient to induce cells into the osteogenic lineage compared to the *in-house* media (compare intensity of the Alizarin Red staining on Figure 31A *vs*. Figure 31B). As expected, the cells cultured in general media (DMEM + 10% Fetal Bovine Serum + 1% Penicillin/Streptomycin + 1% Fungizone) did not stain (negative control) for Alizarin Red (Figure 31C).

Interestingly, as shown on Figures 32-33, both osteogenic medias (*in-house vs*. commercial) successfully induced the fibrotic nodules towards the osteogenic pathway. However, the nodules induced with the commercial media (Figure 33) stained stronger for Alizarin Red compared to the nodules induced with the *in-house* media (Figure 32), which suggests that osteogenic differentiation for 4-weeks was more robustly induced when the commercial media was used on our culture conditions. Also of importance, no significant differences were observed between the treatments with different TGF-beta inhibitors and the ability of the fibrotic nodules to

undergo osteogenic differentiation, independent of the type of osteogenic media used in the induction (Figures 32 and 33).

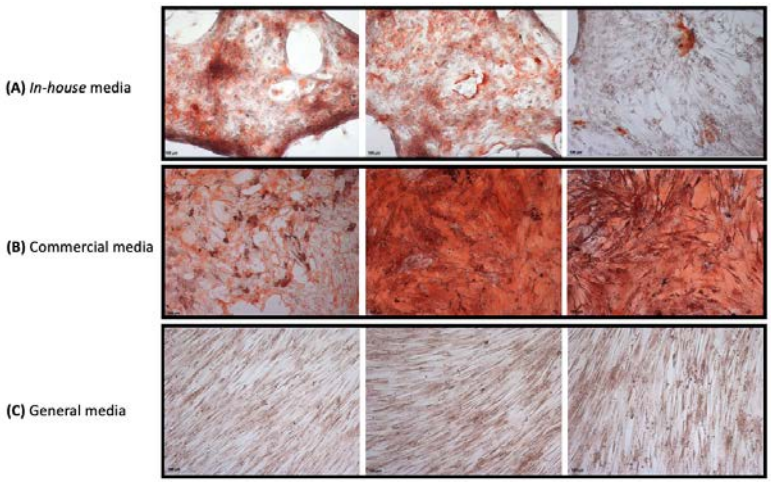

Figure 31 – Mesenchymal progenitor cells cultured in a conventional (monolayer) plate induced to osteogenic differentiation for 4-weeks with **(A)** *in-house* osteogenic media (J Bone Joint Surg Am. 2008;90(11):2390-8) and **(B)** commercially available osteogenic media. **(C)** Cells were cultured in general media (DMEM + 10% Fetal Bovine Serum + 1% Penicillin/Streptomycin + 1% Fungizone) as control. Following differentiation, cells were stained with 1.5% Alizarin Red.

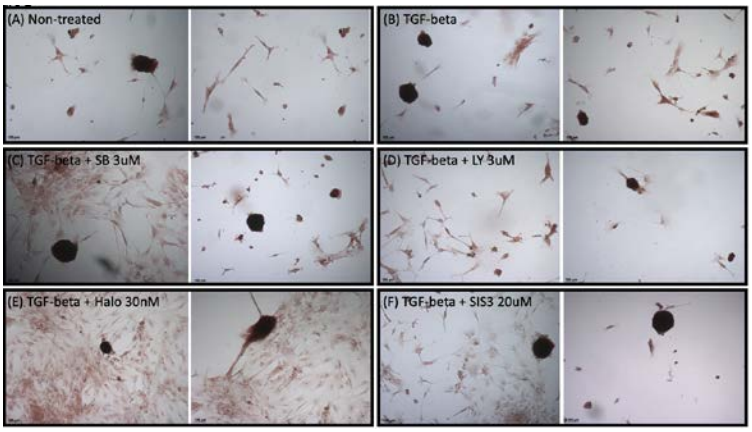

Figure 32 – Mesenchymal progenitor cells treated with TGF-beta for fibrotic nodules formation for 4-days followed by osteogenic differentiation for 4-weeks with *in-house* osteogenic media (J Bone Joint Surg Am. 2008;90(11):2390-8). **(A)** Non-treated control, **(B)** TGF-beta treatment control [10 ng/mL], **(C)** TGF-beta [10 ng/mL] + SB431542 [3uM], **(D)** TGF-beta [10 ng/mL] + LY2157299 [3uM], **(E)** TGF-beta [10 ng/mL] + Halofuginone [30nM] and **(F)** TGF-beta [10 ng/mL] + SIS3 [20uM]. Treatments were performed for 4-days during the fibrotic nodule formation phase. Following differentiation, cells were stained with 1.5% Alizarin Red. SB = SB431542, LY = LY2157299 and Halo = Halofuginone.

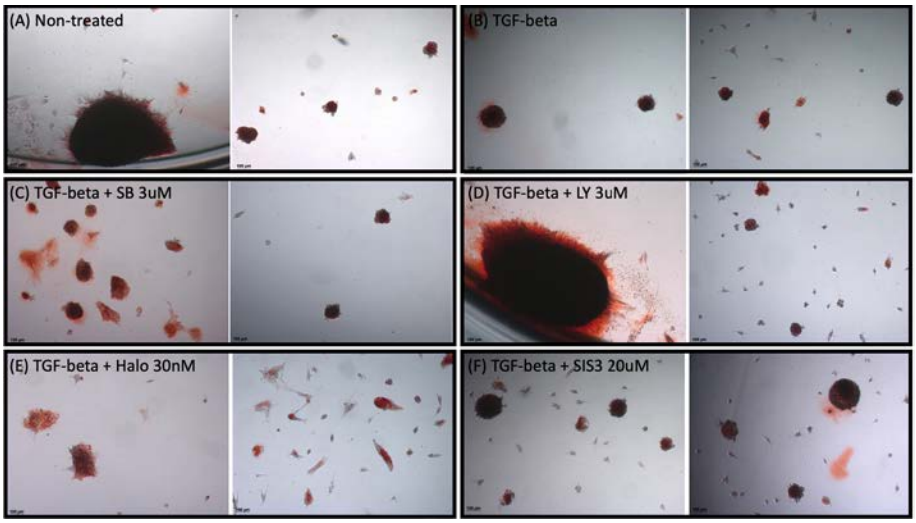

Figure 33 – Mesenchymal progenitor cells treated with TGF-beta for fibrotic nodules formation for 4-days followed by osteogenic differentiation for 4-weeks with ***commercial*** osteogenic media. **(A)** Non-treated control, **(B)** TGF-beta treatment control [10 ng/mL], **(C)** TGF-beta [10 ng/mL] + SB431542 [3uM], **(D)** TGF-beta [10 ng/mL] + LY2157299 [3uM], **(E)** TGF-beta [10 ng/mL] + Halofuginone [30nM] and **(F)** TGF-beta [10 ng/mL] + SIS3 [20uM]. Treatments were performed for 4-days during the fibrotic nodule formation phase. Following differentiation, cells were stained with 1.5% Alizarin Red. SB = SB431542, LY = LY2157299 and Halo = Halofuginone.

We also investigated the differences between the gene expression profile of 6 fibrotic markers (*ACTA2*, *COL1A1*, *FN1*, *SERPINE1*, *MMP9* and *CDH2*) and 3 osteogenic markers (*CBFA1*, *ALP* and *Osteocalcin*) following culture of mesenchymal progenitor cells (MPCs) and treatment with TGF-beta or TGF-beta + TGFB inhibitors in a monolayer plate (conventional culture conditions) or a 3-dimensional commercial polycaprolactone (PCL) nanofiber plate. The commercial PCL nanofiber plate used on these experiments have fibers on a random orientation, which we believe best mimics the fibers formed on the fibrotic/scar tissue following a traumatic injury *in vivo*. As shown on Figures 34-35, treatment with TGF-beta [10 ng/mL] alone consistently increased the fibrotic markers, with the exception of *MMP9.* Interestingly, in many cases higher expression levels were observed on the PCL nanofiber plates compared to regular (monolayer) plates. Also, the addition of TGFB inhibitors consistently down-regulated the expression of *ACTA2*, *COL1A1* and *FN1* (Figure 34). Also of note, only the ALK5 inhibitors (SB431542 and LY2157299) demonstrated an effect on the levels of *SERPINE1* and *CDH2*, while *MMP9* expression levels remained mostly unaffected (Figure 35).

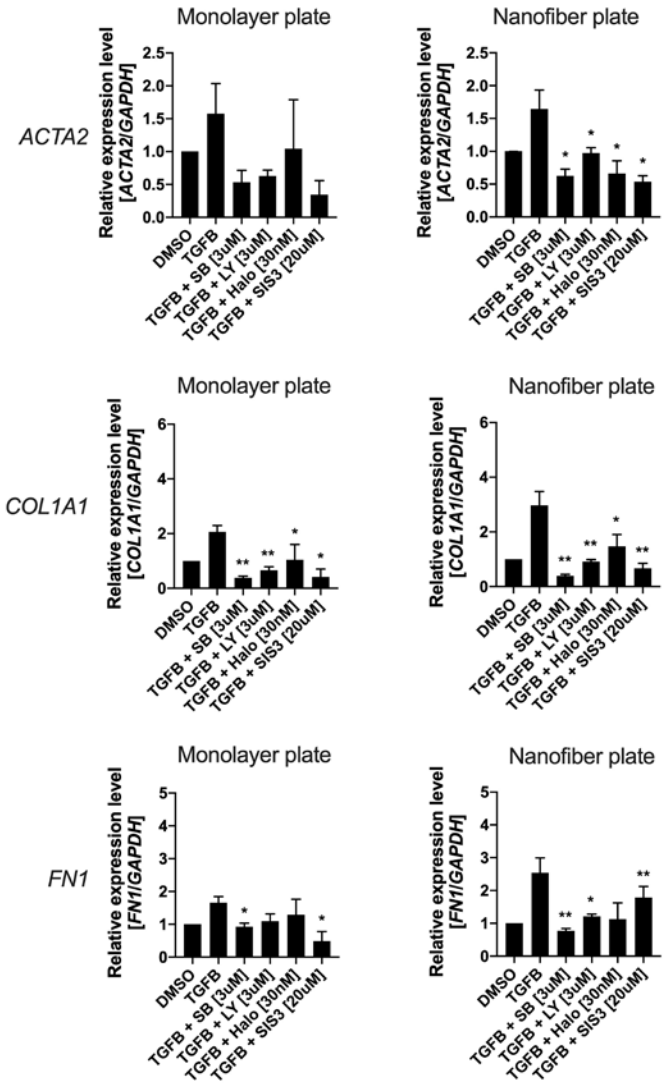

Figure 34 – Quantitative PCR (q-RT-PCR) analysis of the fibrotic markers *ACTA2*, *COL1A1* and *FN1*. MPCs were cultured on regular (monolayer) plates or randomly oriented PCL nanofiber plates and treated with TGF-beta [10 ng/mL] alone (control), TGF-beta [10 ng/mL] + SB431542 [3uM], TGF-beta [10 ng/mL] + LY2157299 [3uM], TGF-beta [10 ng/mL] + Halofuginone [30nM] and TGF-beta [10 ng/mL] + SIS3 [20uM] for 4-days followed by RNA extraction and q-RT-PCR analysis. Gene expression was normalized using *GAPDH* as an internal housekeeping control. DMSO alone was used as vehicle control. Results represent the average of three independent donors. *p<0.05, **p≦0.01, T-test 1-tail. SB = SB431542; LY = LY2157299; Halo = Halofuginone.

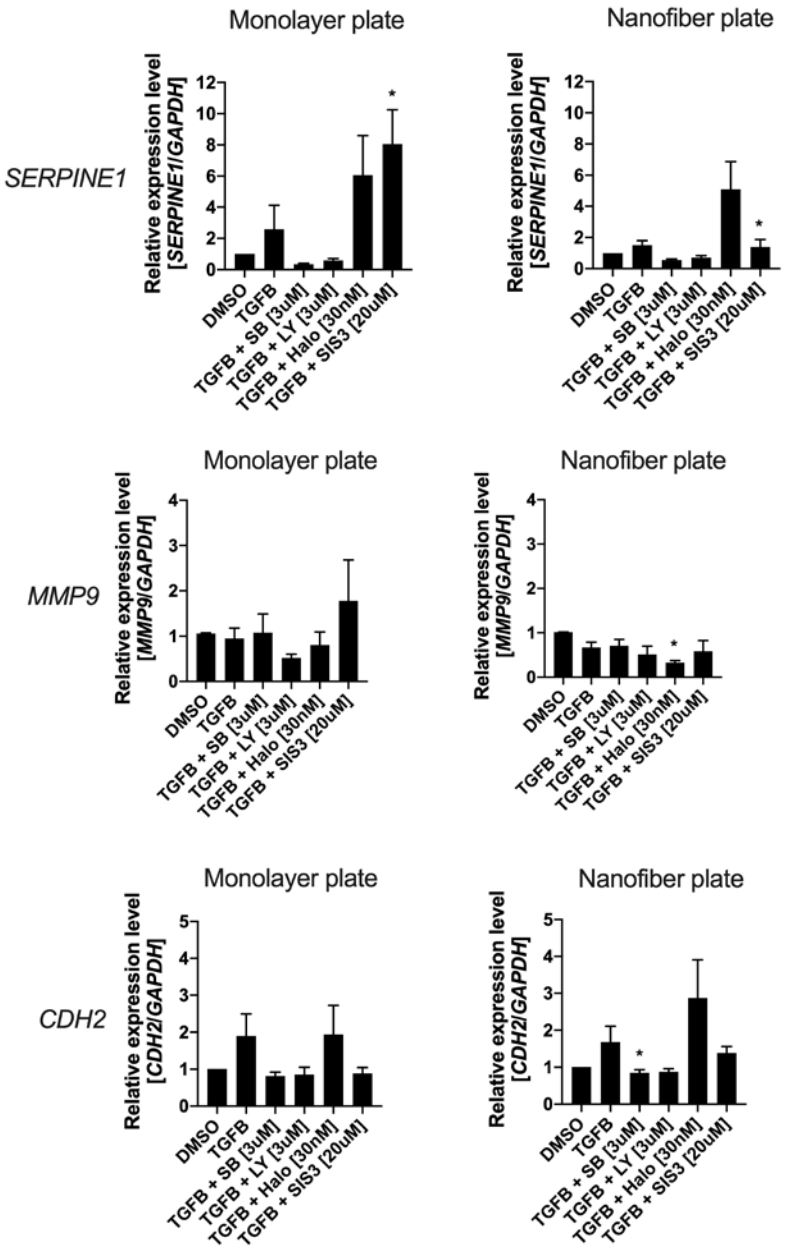

Figure 35 – Quantitative PCR (q-RT-PCR) analysis of the fibrotic markers *SERPINE1*, *MMP9* and *CDH2*. MPCs were cultured on regular (monolayer) plates or randomly oriented PCL nanofiber plates and treated with TGF-beta [10 ng/mL] alone (control), TGF-beta [10 ng/mL] + SB431542 [3uM], TGF-beta [10 ng/mL] + LY2157299 [3uM], TGF-beta [10 ng/mL] + Halofuginone [30nM] and TGF-beta [10 ng/mL] + SIS3 [20uM] for 4-days followed by RNA extraction and q-RT-PCR analysis. Gene expression was normalized using *GAPDH* as an internal housekeeping control. DMSO alone was used as vehicle control. Results represent the average of three independent donors. *p<0.05, T-test 1-tail. SB = SB431542; LY = LY2157299; Halo = Halofuginone.

Additionally, we investigated the expression levels of the osteogenic markers *CBFA1*, *ALP* and *Osteocalcin* in these conditions (monolayer plate vs. nanofiber plate). As shown on Figure 36, both *CBFA1* and *ALP* mRNA levels were higher following treatment with TGF-beta [10 ng/mL], while *Osteocalcin* mRNA levels remained mostly unaffected. Of interest, *CBFA1* levels were consistently down-regulated upon treatment with TGFB inhibitors, while effects on *ALP* and *Osteocalcin* were less consistent between the treatments (Figure 36).

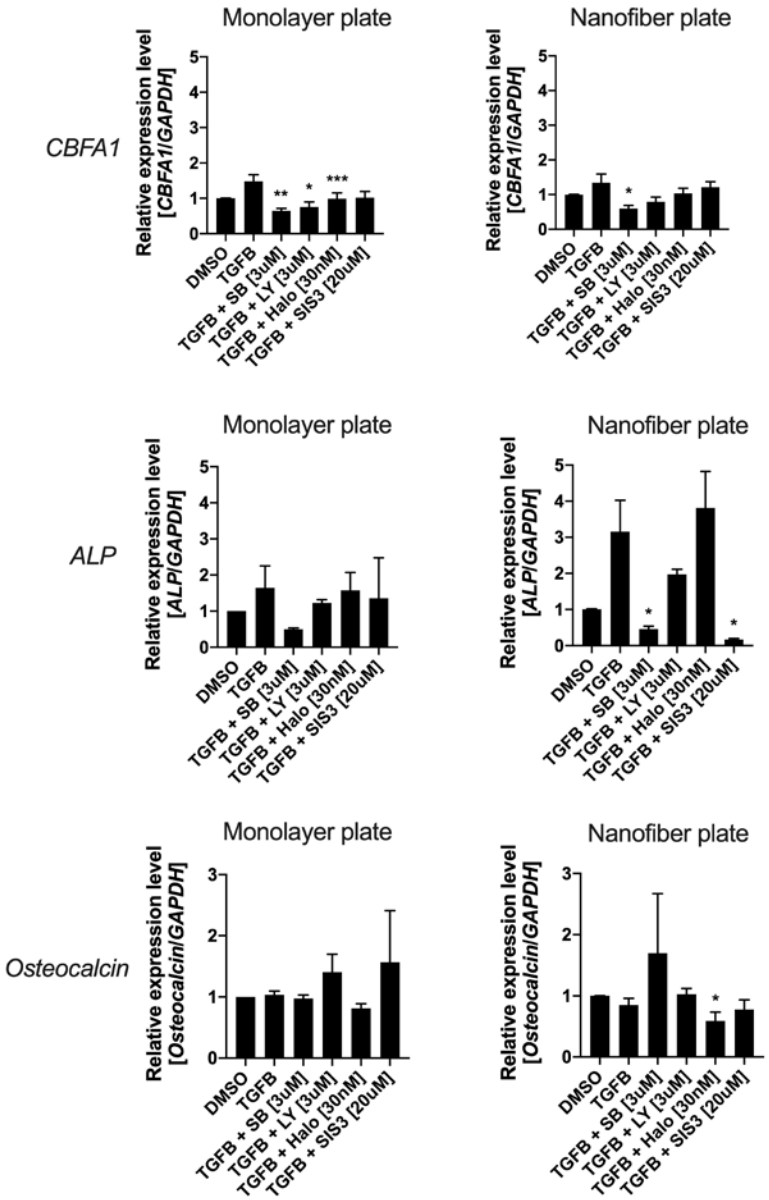

Figure 36 – Quantitative PCR (q-RT-PCR) analysis of the osteogenic markers *CBFA1*, *ALP* and *Osteocalcin*. MPCs were cultured on regular (monolayer) plates or randomly oriented PCL nanofiber plates and treated with TGF-beta [10 ng/mL] alone (control), TGF-beta [10 ng/mL] + SB431542 [3uM], TGF-beta [10 ng/mL] + LY2157299 [3uM], TGF-beta [10 ng/mL] + Halofuginone [30nM] and TGF-beta [10 ng/mL] + SIS3 [20uM] for 4-days followed by RNA extraction and q-

RT-PCR analysis. Gene expression was normalized using *GAPDH* as an internal housekeeping control. DMSO alone was used as vehicle control. Results represent the average of three independent donors. *p<0.05, **p≦0.01, *** p≦0.001, T-test 1-tail. SB = SB431542; LY = LY2157299; Halo = Halofuginone.

For comparison with the TGFB inhibitors, we chose to perform a genetic knockdown of SMAD2/3 on primary MPCs. These experiments aim to compare the effects of a genetic knockdown of SMAD2/3 vs. the small molecule inhibition of SMAD2/3 obtained by the use of the inhibitors. We started these experiments with SMAD3 and performed an initial test to investigate the best technical conditions to perform the SMAD3 knockdown (SMAD3-KD) experiment on MPCs. As shown on Figure 37, several conditions (SMAD3-KD 1ul and 2ul) and reagents (Lipofectamine 2000 and Lipofectamine RNAiMAX 3ul and 4 ul each) were tested for protocol optimization, and the best condition observed (reflected by the highest reduction of SMAD3 levels; Figure 39 right panel) consisted of SMAD3-KD 2ul + Lipofectamine RNAiMAX 3ul (dark gray bars). Interestingly, consistently Lipofectamine RNAiMAX (Figure 39 right panel, dark gray and light gray bars) showed better results compared to Lipofectamine 2000 (Figure 37 right panel, black and white bars). As expected, SMAD2 levels were not down-regulated by the SMAD3-KD, which demonstrated the specificity of the siRNA used in our study (Figure 37 left panel).

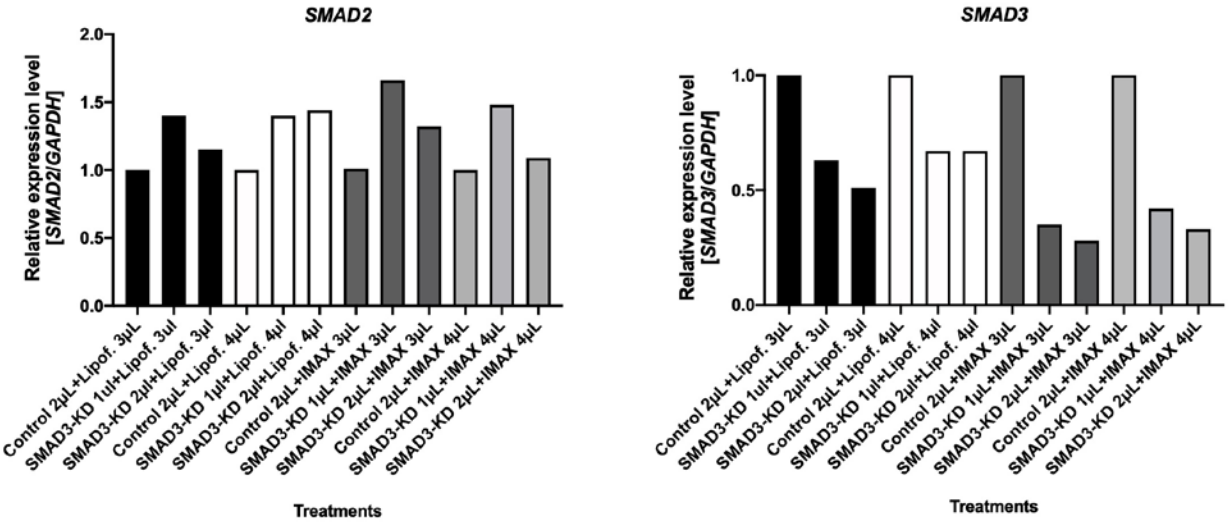

Figure 37 – Quantitative PCR (q-RT-PCR) analysis for *SMAD2* and *SMAD3* 4-days following *SMAD3* knockdown (SMAD3-KD) in different experimental conditions (Lipof. = Lipofectamine 2000; IMAX = Lipofectamine RNAiMAX). A scramble was used as transfection control (identified in the figure as Control). SMAD3-KD was tested in two different volumes (1ul and 2ul), Lipofectamine 2000 was tested in two different volumes (3ul and 4ul), and Lipofectamine RNAiMAX was tested in two different volumes (3ul and 4ul). Gene expression was normalized using *GAPDH* as an internal housekeeping control. Results represent the average of three independent reactions from one donor.

Finally, to further investigate the effects of the SMAD3-KD on this experiment, we analyzed the expression of 4 fibrotic markers (*ACTA2*, *COL1A1, FN1* and *CDH2*) and 3 osteogenic markers (*CBFA1, ALP* and *Osteocalcin*) following SMAD3-KD. As shown on Figure 38, minor reductions on the expression levels of *COL1A1, FN1*, *CDH2, ALP* and *Osteocalcin* were observed, while a slight increase was observed on the mRNA levels of *ACTA2* and *CBFA1*. Importantly, these experiments are preliminary results, and were not performed with the addition of TGFB, which we have previously shown to stimulate the expression of fibrotic markers in primary MPCs.

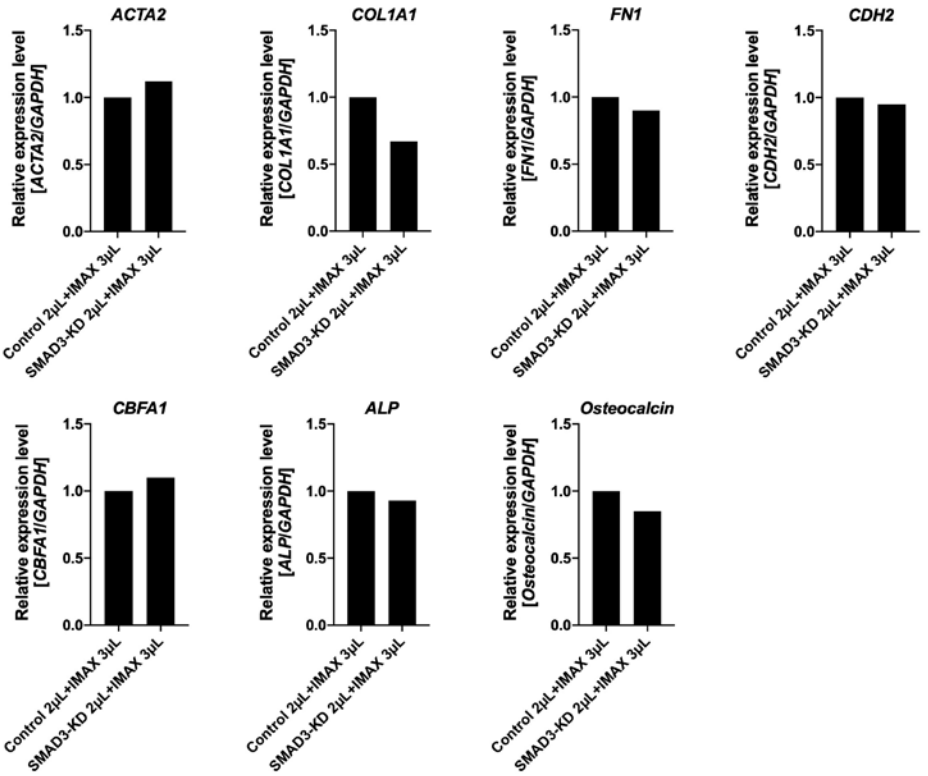

Figure 38 – Quantitative PCR (q-RT-PCR) analysis of the fibrotic markers *ACTA2*, *COL1A1, FN1* and *CDH2*, and osteogenic markers *CBFA1, ALP* and *Osteocalcin* following SMAD3 knockdown (SMAD3-KD). SMAD3-KD was performed with 3ul of Lipofectamine RNAiMAX and a scramble was used as transfection control (identified in the figure as Control) for 4-days followed by RNA extraction and q-RT-PCR analysis. Gene expression was normalized using *GAPDH* as an internal housekeeping control. Results represent the average of three independent reactions from one donor.

Following these preliminary results, knockdown optimization was performed and down-regulation of SMAD2 and SMAD3 was confirmed by q-RT-PCR analysis (Figure 39) and Western blot (Figure 40).

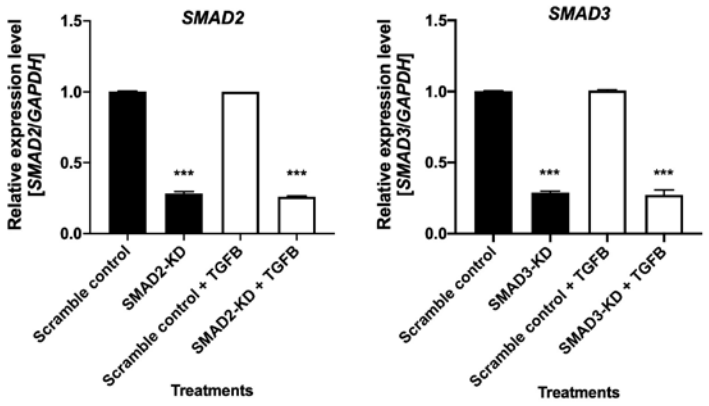

Figure 39 – Quantitative PCR (q-RT-PCR) analysis for *SMAD2* and *SMAD3* 48h following *SMAD2* knockdown (SMAD2-KD) or *SMAD3* knockdown (SMAD3-KD) as indicated in the absence or presence of TGF-beta (TGFB). Gene expression was normalized using *GAPDH* as an internal housekeeping control. Scramble transfection was used as control. Results represent the average of 4 independent donors. ***p<0.001, T-test 1-tail.

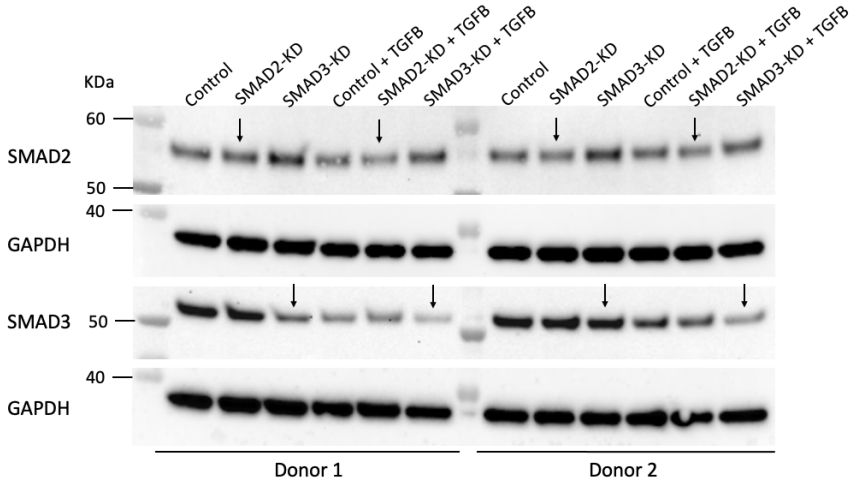

Figure 40 – Western blot analysis for SMAD2 and SMAD3 48h following SMAD2 knockdown (SMAD2-KD) or SMAD3 knockdown (SMAD3-KD) as indicated. GAPDH was used as loading control. Representative results from 2 independent donors are shown.

Upon confirmation of the knockdowns, we investigated the effects of SMAD2 knockdown (SMAD2-KD) and SMAD3 knockdown (SMAD3-KD) in the expression of fibrotic and osteogenic markers. As shown on Figures 41-42, some fibrotic markers (*ACTA2*, *COL1A1*, *COL3A1* and *MMP9*) were significantly down-regulated upon SMAD2-KD and SMAD3-KD, while *CDH2*, *MMP2* and *VIM* were significantly down-regulated only upon SMAD3-KD. In the presence of TGF-beta, *COL1A1*, *COL1A3*, *FN1* and *VIM* were significantly down-regulated upon SMAD2-KD and SMAD3-KD, while *MMP2* was significantly down-regulated only upon SMAD2-KD.

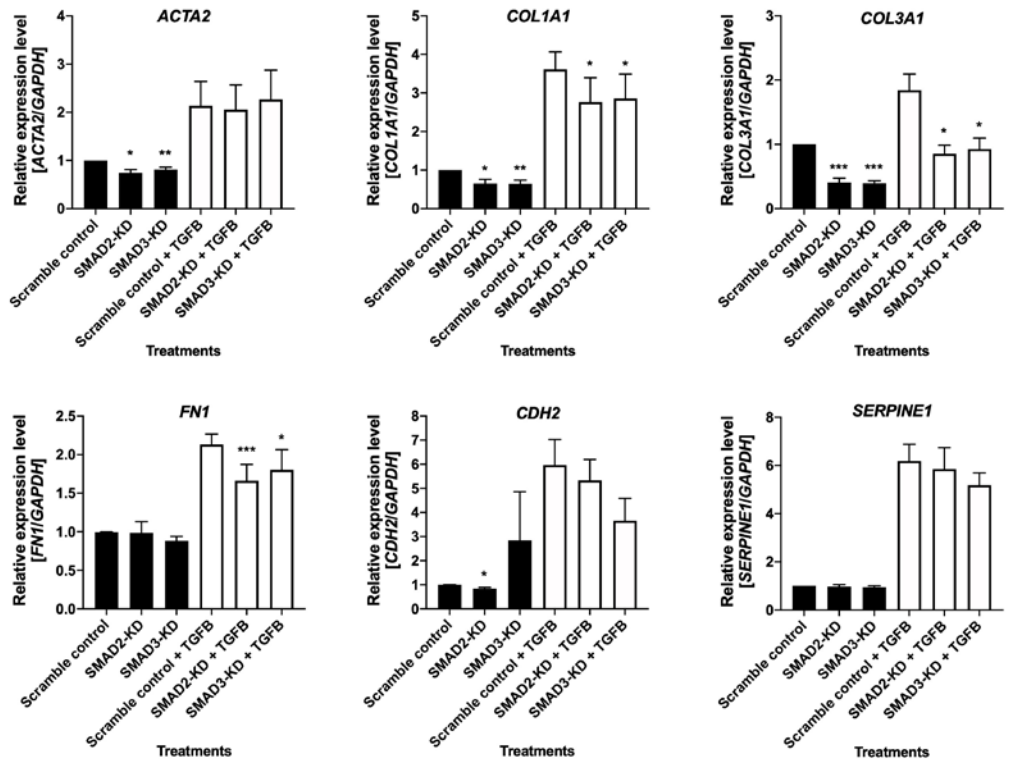

Figure 41 – Quantitative PCR (q-RT-PCR) analysis of the fibrotic markers *ACTA2*, *COL1A1, COL1A3, FN1, CDH2* and *SERPINE1* 48h following *SMAD2* knockdown (SMAD2-KD) or *SMAD3* knockdown (SMAD3-KD). Gene expression was normalized using *GAPDH* as an internal housekeeping control. Scramble transfection was used as control. Results represent the average of 4 independent donors. *p<0.05, **p<0.01, ***p<0.001, T-test 1-tail.

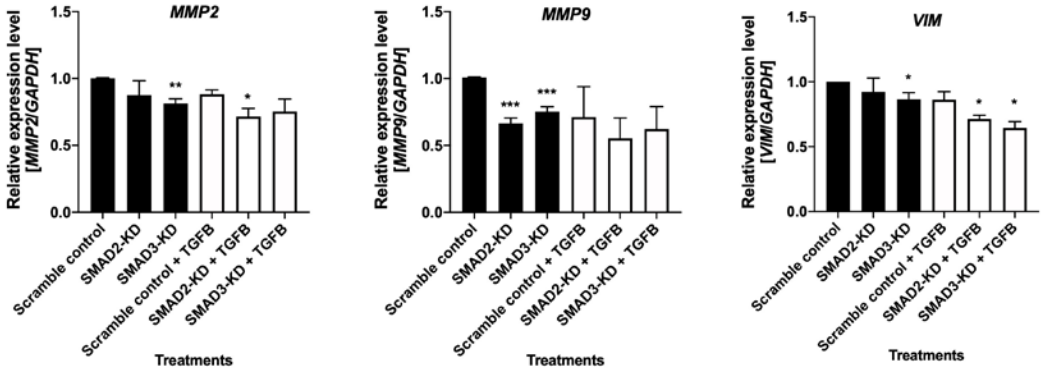

Figure 42 – Quantitative PCR (q-RT-PCR) analysis of the fibrotic markers *MMP2*, *MMP9* and *VIM* 48h following *SMAD2* knockdown (SMAD2-KD) or *SMAD3* knockdown (SMAD3-KD). Gene expression was normalized using *GAPDH* as an internal housekeeping control. Scramble transfection was used as control. Results represent the average of 4 independent donors. *p<0.05, **p<0.01, ***p<0.001, T-test 1-tail.

Also, the osteogenic markers *CBFA1*, *ALP* and *Osteocalcin* were investigated following SMAD2-KD and SMAD3-KD. As shown on Figure 43, no significant effects were observed on *CBFA1*, while only *ALP* was down-regulated upon SMAD3-KD in the absence of TGF-beta. In addition, *ALP* was down-regulated upon both SMAD2-KD and SMAD3-KD, while *Osteocalcin* was down-regulated only upon SMAD2-KD in the presence of TGF-beta.

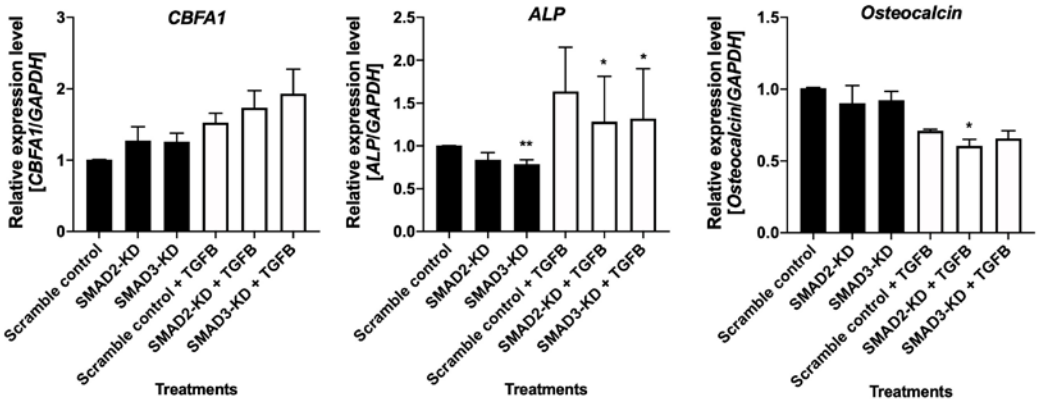

Figure 43 – Quantitative PCR (q-RT-PCR) analysis of the osteogenic markers *CBFA1*, *ALP* and *Osteocalcin* 48h following *SMAD2* knockdown (SMAD2-KD) or *SMAD3* knockdown (SMAD3-KD). Gene expression was normalized using *GAPDH* as an internal housekeeping control. Scramble transfection was used as control. Results represent the average of 4 independent donors. *p<0.05, **p<0.01, T-test 1-tail.

Finally, we focused our efforts investigating the effects of the TGF-beta inhibitors (SB431542, LY2157299, Halofuginone and SIS3) treatments on the osteogenic markers *ALP*, *CBFA1* and *Osteocalcin* during osteogenic differentiation. MPCs were treated with the TGF-beta inhibitors for 4-days followed by osteogenic differentiation. As shown on Figure 44, *CBFA1* was significantly down-regulated upon treatments with LY2157299 and Halofuginone, while *Osteocalcin* was down-regulated only upon treatment with SB431542.

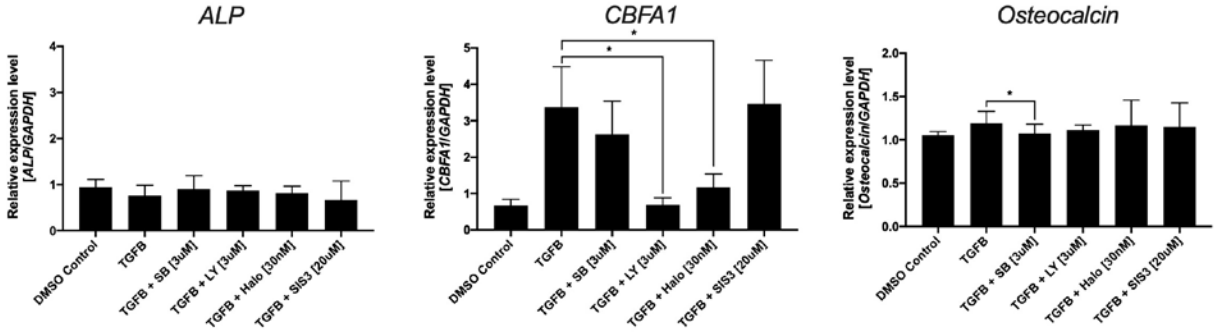

Figure 44 – Quantitative PCR (q-RT-PCR) analysis of the osteogenic markers *ALP*, *CBFA1* and *Osteocalcin* following treatment with the TGF-beta inhibitors for 4-days + 1-week of osteogenic differentiation. Gene expression was normalized using *GAPDH* as an internal housekeeping

control. DMSO was used as a vehicle control. Results represent the average of 3 independent donors. *p<0.05, T-test 1-tail.

We continued osteogenic differentiation up to 4-weeks, with a timepoint every week. As shown on Figure 45, *ALP* was up-regulated upon LY2157299 treatment, while *CBFA1* was down-regulated upon both SB431542 and LY2157299 treatments on week 2 of osteogenic differentiation.

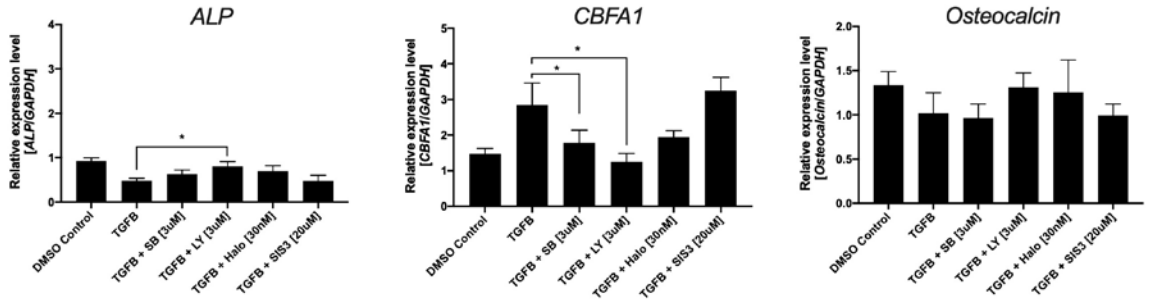

Figure 45 – Quantitative PCR (q-RT-PCR) analysis of the osteogenic markers *ALP*, *CBFA1* and *Osteocalcin* following treatment with the TGF-beta inhibitors for 4-days + 2-weeks of osteogenic differentiation. Gene expression was normalized using *GAPDH* as an internal housekeeping control. DMSO was used as a vehicle control. Results represent the average of 3 independent donors. *p<0.05, T-test 1-tail.

Following 3-weeks of osteogenic differentiation, only *CBFA1* was significantly up-regulated upon treatment with SIS3 (Figure 46). Finally, following 4-weeks of osteogenic differentiation *ALP* was down-regulated upon LY2157299 and SIS3 treatments, while *Osteocalcin* was down-regulated only upon LY2157299 treatment (Figure 47).

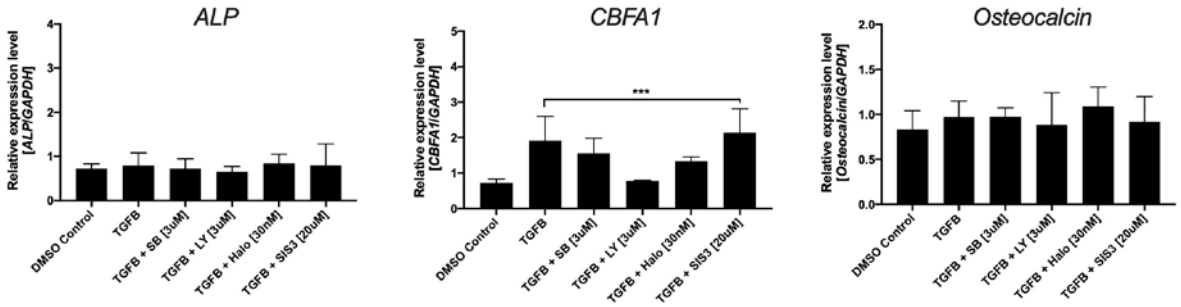

Figure 46 – Quantitative PCR (q-RT-PCR) analysis of the osteogenic markers *ALP*, *CBFA1* and *Osteocalcin* following treatment with the TGF-beta inhibitors for 4-days + 3-weeks of osteogenic differentiation. Gene expression was normalized using *GAPDH* as an internal housekeeping control. DMSO was used as a vehicle control. Results represent the average of 3 independent donors. *p<0.05, T-test 1-tail.

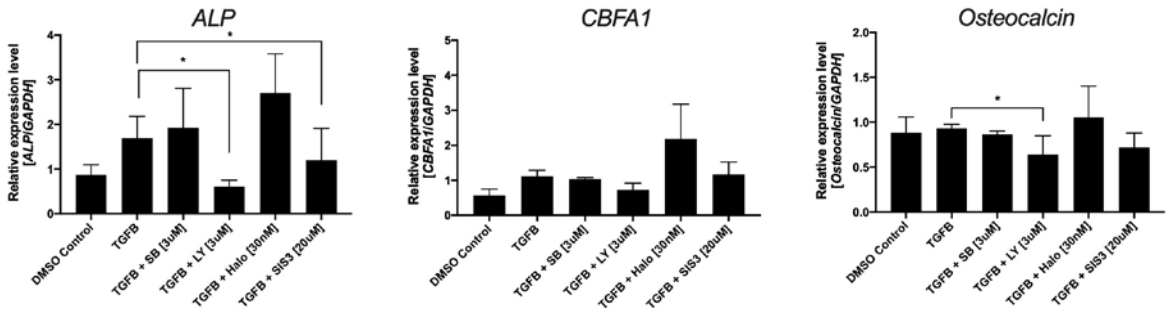

Figure 47 – Quantitative PCR (q-RT-PCR) analysis of the osteogenic markers *ALP*, *CBFA1* and *Osteocalcin* following treatment with the TGF-beta inhibitors for 4-days + 4-weeks of osteogenic differentiation. Gene expression was normalized using *GAPDH* as an internal housekeeping control. DMSO was used as a vehicle control. Results represent the average of 3 independent donors. *p<0.05, T-test 1-tail.

In addition to the in vitro studies shown above, animal studies were performed by the sub-award PI Dr. Vincent Pellegrini Jr. All animal procedures were performed under approved appropriate protocols by the Institutional Animal Care and Use Committee at the Medical University of South Carolina. Sprague-Dawley rats (n=160 as follows: n=80 blast amputation group and n=80 no-trauma control group) were first anesthetized with ketamine (80 mg/kg) and xylazine (7 mg/kg) delivered intraperitoneally, and pre-blast doses of enrofloxacin (5 mg/kg) and buprenorphine (0.05 mg/kg) were administered subcutaneously for antisepsis and analgesia, respectively. The blast setup consisted of a 12x12x2-inch aluminum platform welded above a 2x2x2-foot steel tank. The platform had a hole through its center that was 2.5 inches in diameter were the animals were secured with two industrial sized Velcro straps across the chest and abdomen. The rat was positioned sternally (ventrally) onto the platform and the designated hindlimb was held exposed over the hole in the platform, 5-10 millimeters distal to the knee joint. The tank was filled with water up to a level of 1 inch beneath the bottom of the platform. The Pentaerythritol tetranitrate (PETN) explosive was submerged 0.5 inch beneath the surface of the water, and directly beneath the center of the hole in the platform, at a total stand-off distance of 3.5 inches from the top of the platform. PETN detonation caused a column of water to travel through the opening in the platform and amputate the exposed extremity. Immediately afterwards, injured rats were transferred to sterile field for wound management and primary surgical closure. A detailed description of the blast setup, blast, surgical closure and post blast care has been previously reported by Dr. Vincent Pellegrini's group. Rodents were divided into four treatment groups (40 animals per group: 20 blast amputation group and n=20 no-trauma control group) to test the effects of the following TGFß inhibitors [low dose, medium dose and high treatment dose, respectively]: SB431542 [5 ug/g, 10 ug/g and 30 ug/g bodyweight], Galunisertib (LY2157299) [16 ug/g, 30 ug/g and 36 ug/g bodyweight], Halofuginone [2.5 ug/g, 5 ug/g and 10 ug/g bodyweight] and SIS3 [2 ug/g, 10 ug/g and 50 ug/g bodyweight]. Each group included a set of 10 animals (5 blast amputation group and 5 no-trauma control group) each as a control (no drug administered) group (Figure 48).

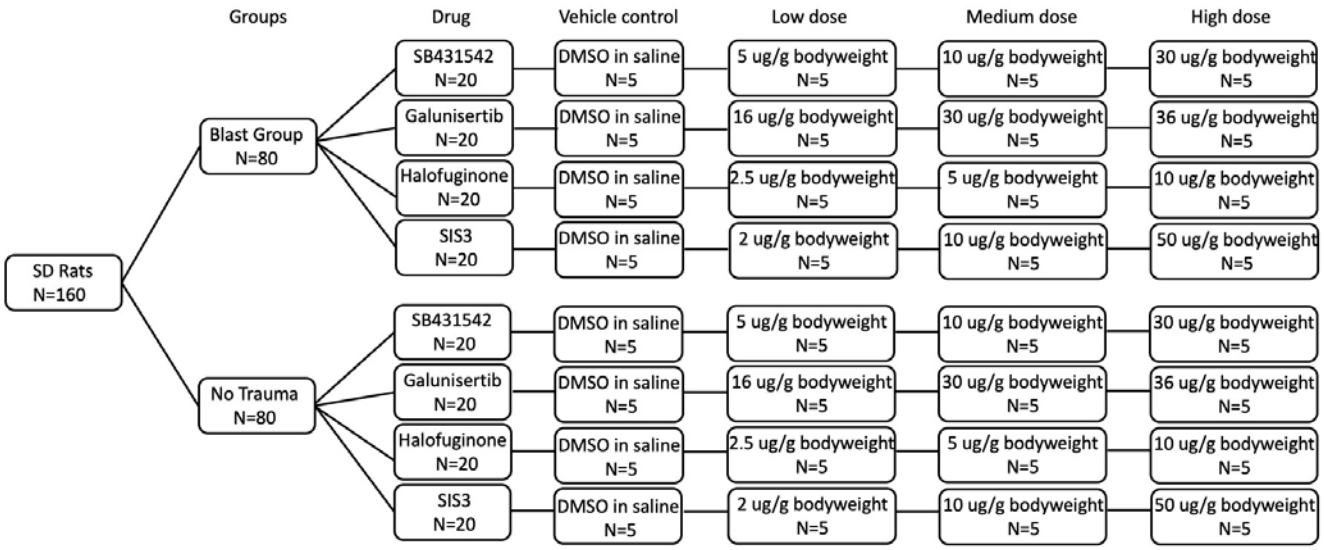

Figure 48 – Schematic representation of the rat blast and no-trauma control treatment groups.

For each treatment condition, two animals were sacrificed at a 2-weeks timepoint and three animals were sacrificed at a 4-months timepoint, and the hindlimb was fixed in a 10% formalin solution (Sigma-Aldrich, St. Louis, MO). In the acute post-operative period, rats were monitored for signs of distress, and given a 5-day course of buprenorphine (0.05 mg/kg administered subcutaneously twice a day) and enrofloxacin (5 mg/kg administered subcutaneously twice a day). Radiographs of the amputated limbs were performed with a digital Faxitron radiography machine (Faxitron X-Ray LLC, Lincolnshire, IL). The 4 months survival groups underwent routine X-ray assessments beginning after the first month following amputation for 2-week intervals for the remainder of their survival. Two independent reviewers graded the extent of heterotopic ossification (HO) visualized on radiographs. HO was graded on a scale of 0-2, whereby a grade of 0 represented no HO, a grade of 1 represented mild HO (defined as >0 but less than 25% of the diaphyseal diameter), and a grade of 2 represented moderate to severe HO (defined as more than >25% of the diaphyseal diameter). This grading scale was modified from Hoyt et al. (Journal of Orthopaedic Trauma 34(12):2020). for this study. Grades for each radiograph were averaged to give a final score for each image. As shown on Figure 49, trends to a lower x-ray assessment score (lower HO grading scale) were observed upon SB431542 treatment in all timepoints, Halofuginone treatment on the 1 month + 1.5 months timepoint as well as upon SIS3 treatment on all timepoints until 3.5 months after injured.

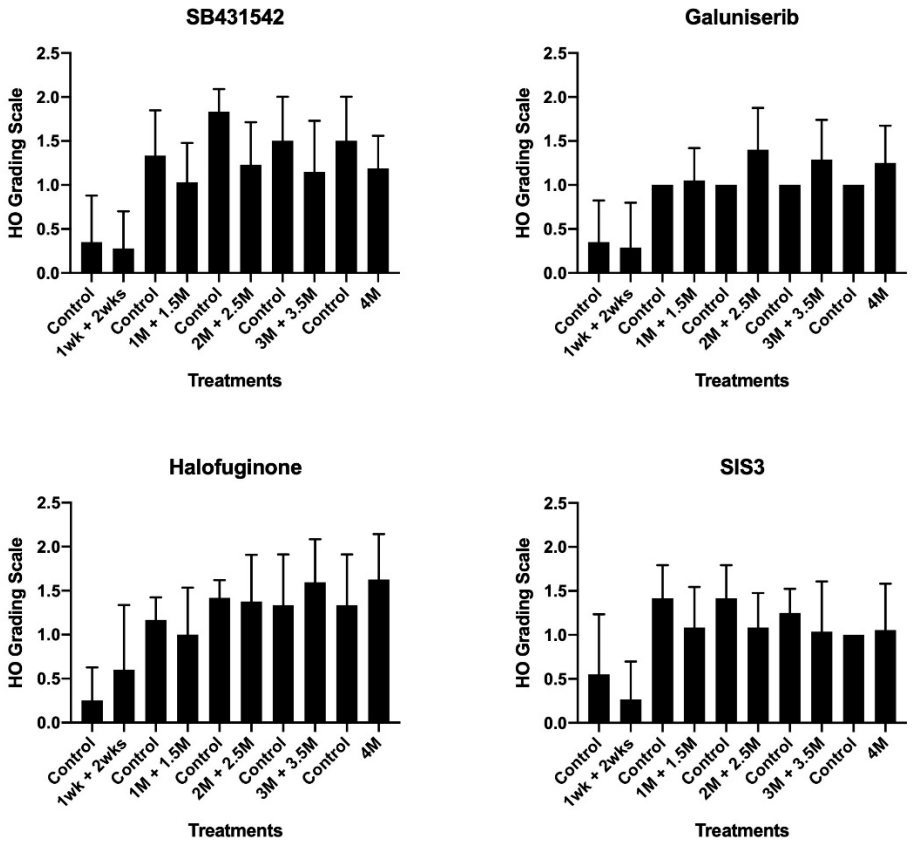

Figure 49 – X-ray assessment score (HO grading scale) following injury on Sprague-Dawley rats. Two independent reviewers graded the extent of heterotopic ossification (HO) visualized on radiographs. HO was graded on a scale of 0-2, whereby a grade of 0 represented no HO, a grade of 1 represented mild HO (defined as >0 but less than 25% of the diaphyseal diameter), and a grade of 2 represented moderate to severe HO (defined as more than >25% of the diaphyseal diameter). This grading scale was modified from Hoyt et al. (Journal of Orthopaedic Trauma 34(12):2020). for this study. Grades for each radiograph were averaged to give a final score for each image. Results represent the average of 2 independent animals for the 2-weeks timepoint and 3 independent animals for all the remaining timepoints up to 4-months. 1wk + 2wks = 1-week and 2-weeks timepoints (combined); 1M + 1.5M = 1 month and 1.5 months timepoints (combined); 2M + 2.5M = 2 months and 2.5 months timepoints (combined); 3M + 3.5M = 3 months and 3.5 months timepoints (combined); 4M = 4 months timepoint.

4. IMPACT:

Musculoskeletal injuries sustained in recent military conflicts have been notable for their number and complexity. Our group has studied this condition in combat related injuries for the greater part of the last decade and we have focused on the earliest and most basic parts of the process to gain insight into the key cell and molecular events leading to heterotopic ossification (HO) formation which is disfiguring, painful and functionally debilitating. Our efforts have enabled us to identify a population of cells that we feel are integral to the process of HO formation, a set

of growth factors that are dysregulated in the healing response and a structural microenvironment which may lead stem cells to an undesirable cell fate. Together these components of wound healing identified in combat-related extremity injuries suggest that over stimulation of a specific fibrotic pathway may be one of the key triggers that initiates these undesirable healing events. This study capitalizes on the years of research devoted to studying these traumatic war wounds and uses a pre-clinical model to help translate the basic science findings into a new clinical treatment. The result will be improved functional recovery after traumatic musculoskeletal injuries for our injured servicemembers.

5. CHANGES/PROBLEMS:

As it is well-known, for several months during the year of 2020 we worked under COVID-19 pandemic restrictions. We followed Phase 1 and Phase 2 re-opening safety guidelines from USUHS during the pandemic. Delays on experimental procedures were observed, as well as more limited opportunities to submit abstracts and present our work in scientific conferences.

6. PRODUCTS:

Publications, conference papers, and presentations

Journal publications:

1. de Vasconcellos JF, Zicari S, Fernicola SD, Griffin DW, Ji Y, Shin EH, Jones P, Christopherson GT, Bharmal H, Cirino C, Nguyen T, Robertson A, Pellegrini V, Nesti LJ. In vivo model of human post-traumatic heterotopic ossification demonstrates early fibroproliferative signature. **J Transl Med**. 2019;17(1):248.

2. de Vasconcellos JF, Jackson WM, Dimtchev A, Nesti LJ. A microRNA Signature for Impaired Wound-Healing and Ectopic Bone Formation in Humans. **J Bone Joint Surg Am**. 2020;102(21):1891-1899.

3. Dingle M, Fernicola SD, de Vasconcellos JF, Zicari S, Daniels C, Dunn JC, Dimtchev A, Nesti LJ. Characterization of traumatized muscle-derived multipotent progenitor cells from low-energy trauma. **Stem Cell Res Ther.** 2021;12(1):6.

4. Christopherson GT, de Vasconcellos JF, Dunn JC, Griffin DW, Jones PE, Nesti LJ. Three-dimensional modeling of the structural microenvironment in post-traumatic war wounds. **Tissue Eng Regen Med.** 2021 Aug 7. doi: 10.1007/s13770-021-00355-y. Online ahead of print.

Other publications, conference papers, and presentations:

Oral presentations:

1. de Vasconcellos JF, Zicari S, Buckley T, Fernicola S, Dimtchev A, Nesti LJ. Investigating the underlying molecular mechanisms involved in post-traumatic heterotopic ossification. 60th Society of Military Orthopaedic Surgeons (SOMOS) Annual Meeting, 2018. Rapid Fire presentation.

2. Dingle M, Fernicola SD, Zicari S, Yaszemski AK, de Vasconcellos JF, Nesti LJ. Traumatized muscle derived multipotent progenitor cells from low energy fractures. Walter Reed National Military Center Research Symposium, 2019. Finalist for the Robert A. Phillips Award Competition.

3. de Vasconcellos JF, Dingle M, Dimtchev A, Desraj C, Piscoya A, Nesti LJ. Effects of a targeted-therapy approach for post-traumatic heterotopic ossification. 61th Society of Military Orthopaedic Surgeons (SOMOS) Annual Meeting, 2019.

4. Piscoya A, Desraj C, Dingle M, de Vasconcellos JF, Dimtchev A, Nesti LJ. Inhibition of TGF-beta signaling modulates fibrosis in a model of human post-traumatic heterotopic ossification. Walter Reed National Military Center Research Symposium, 2020. Finalist for the Robert A. Phillips Award Competition.

5. de Vasconcellos JF, Dingle M, Piscoya A, Desraj C, Putko R, Bedrin M, Dimtchev A, Nesti LJ. TGF-beta-targeting as a novel therapeutic strategy for post-traumatic heterotopic ossification. 62th Society of Military Orthopaedic Surgeons (SOMOS) Annual Meeting, 2020.

6. de Vasconcellos JF, Dingle M, Piscoya A, Desraj C, Putko R, Bedrin M, Dimtchev A, Nesti LJ. A Novel Therapeutic Strategy in the Prevention of Post-traumatic Heterotopic Ossification: Targeting the TGF-beta Pathway. 74th Annual Meeting Virginia Orthopaedic Society, virtual conference, 2021. Awarded Best Oral presentation from the Conference.

Poster presentations:

1. de Vasconcellos JF, Dingle M, Dimtchev A, Nesti LJ. Investigating the expression of fibrotic markers upon TGF-beta targeted-therapies in a cellular model of post-traumatic heterotopic ossification. Orthopaedic Research Society Annual Meeting, 2019.

2. de Vasconcellos JF, Dingle M, Dimtchev A, Nesti LJ. Effects of TGF-beta targeted-therapies in an *in vitro* model of post-traumatic heterotopic ossification. Military Health System Research Symposium, 2019.

3. de Vasconcellos JF, Dingle M, Dimtchev A, Nesti LJ. Effects of TGF-beta targeted-therapies in primary traumatized muscle derived multipotent progenitor cells as a model of human post-traumatic heterotopic ossification. 5th Stem Cell Biology Meeting from Cold Spring Harbor Laboratory, 2019.

4. de Vasconcellos JF, Dingle M, Dimtchev A, Desraj C, Piscoya A, Nesti LJ. Inhibition of TGF-beta signaling in a cellular model of human post-traumatic heterotopic ossification. American Society for Cell Biology Annual Meeting, 2019.

5. de Vasconcellos JF, Dingle M, Desraj C, Piscoya A, Dimtchev A, Nesti LJ. TGF-beta signaling inhibition modulates fibrosis in a model of human post-traumatic heterotopic ossification. Orthopaedic Research Society Annual Meeting, 2020.

7. PARTICIPANTS & OTHER COLLABORATING ORGANIZATIONS

Name: Leon Nesti
Project Role: PI
Nearest person month worked:4.8
Contribution to Project: no change

Name: Jaira Ferreira de Vasconcellos
Project Role: Research Scientist
Nearest person month worked: 48
Contribution to Project: Tasks 1, 2 and 3; scientific oversight

Name: Sonia Zicari
Project Role: Research Scientist
Nearest person month worked: 24
Contribution to Project: Task 1

Name: Noreen Gervasi
Project Role: Translational Scientist
Nearest person month worked: 36
Contribution to Project: Task 2 and 3

Name: Nicholas Kramer
Project Role: Research Associate
Nearest person month worked: 24
Contribution to Project: Task 1

Name: Alexander Dimtchev
Project Role: Senior Technician
Nearest person month worked: 48

Contribution to Project: Tasks 1-3

Name: Dennis Taylor
Project Role: Program Manager
Nearest person month worked: 24
Contribution to Project: Management oversight

Name: Vincent Pellegrini, Jr.
Project Role: Sub award PI
Nearest person month worked: 48
Contribution to Project: Sub award performance

8. SPECIAL REPORTING REQUIREMENTS

None

9. APPENDICES:

None

10. QUAD CHART:

Novel anti-fibrotic strategies in the targeted treatment and prevention of post-traumatic Heterotopic Ossification and enhancement of post-traumatic tissue regeneration.

Opportunity: W81XWH-17-2-0009 **Log:** BA150280

PI: LTC Leon Nesti M.D. Ph.D. **Org:** USU/HJF **Proposal Amount:** $1,992,386

Summary: We hypothesize that interrupting this TGF-b1 mediated signaling process at the level of Smad protein activation will suppress the fibroproliferative response and reduce or eliminate the formation of HO. We propose a preclinical trial to investigate the effect of specifically blocking the activation of the TGF-b1 intracellular signaling proteins, SMAD2 and SMAD3, on the development of posttraumatic HO using the inhibitors SB431542, Galunisertib, SIS3, and Halofuginone.

Aim 1 To assess the efficacy of SB431542, Galunisertib, SIS3, and Halofuginone treatment in preventing fibrosis in a cell culture model.

Aim 2 To assess the efficacy of SB431542, Galunisertib, SIS3, and Halofuginone based therapy in preventing fibrosis and ectopic bone formation in an animal model.

Aim 3 To assess the effectiveness of SB431542, Galunisertib, SIS3, and Halofuginone in promoting muscle regeneration.

Muscle Fibrosis & HO Mediattion

Muscle Trauma → *MPCs* → *Myofibroblasts* → *Myofibroblast Proliferation* → ***Fibrosis HO***

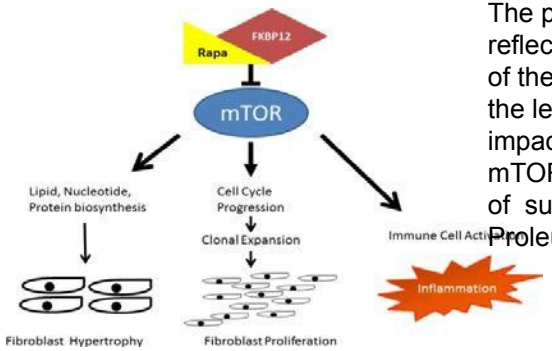

The progression along the top reflects the working hypothesis of the project while the figure to the left shows the known impact of Rapamyacin on mTOR and supports our choice of supplementing with Proleukin

Accomplishment: Animal studies completed; pathology analyses in progress

Timeline and Cost

Activities CY	17	18	19	20	21
Dosing and in-vitro studies					
Small Animal Studies					
Data Analysis					
Publications and closeout					
Estimated Budget ($K)	$498	$664	$413	$177	$239

Updated: 09/03/2021

Goals/Milestones

- ☐ **CY17 Goal** – IACUC Submission, dosing and in vitro studies
- ☐ **CY18 Goals** – Complete In vitro studies and start small animal study
- ☐ **CY19 Goals** - Data Analysis, Publication
- ☐ CY20 Goals – Data Analysis, Publication
- ☐ CY21 Goals – Data analysis, Report and Closeout

Endpoint: To reduce fibrosis and subsequent osteogenesis in a cell culture model and HO formation in a blast injury rat model.

Comments/Challenges/Issues/Concerns: Sub-awardee Dr. Pellegrini moved to Dartmouth College; resumed work upon approval by sponsor. Prime PI, Dr. Nesti is supportive of continuation of his move.

Budget Expenditure to Date:
Projected Expenditure: $1.992M
Actual Expenditure: $1.990,718.69.